REVIEW

Check for updates

Advances in colorimetric biosensors of exosomes: novel approaches based on natural enzymes and nanozymes

Zhonghao Sun,[a] Binmao Zhang,[a] Hangjia Tu,[a] Chuye Pan,[b] Yujuan Chai*[a] and Wenwen Chen [iD] *[a]

Exosomes are 30–150 nm vesicles derived from diverse cell types, serving as one of the most important biomarkers for early diagnosis and prognosis of diseases. However, the conventional detection method for exosomes faces significant challenges, such as unsatisfactory sensitivity, complicated operation, and the requirement of complicated devices. In recent years, colorimetric exosome biosensors with a visual readout underwent rapid development due to the advances in natural enzyme-based assays and the integration of various types of nanozymes. These synthetic nanomaterials show unique physiochemical properties and catalytic abilities, enabling the construction of exosome colorimetric biosensors with novel principles. This review will illustrate the reaction mechanisms and properties of natural enzymes and nanozymes, followed by a detailed introduction of the recent advances in both types of enzyme-based colorimetric biosensors. A comparison between natural enzymes and nanozymes is made to provide insights into the research that improves the sensitivity and convenience of assays. Finally, the advantages, challenges, and future directions of enzymes as well as exosome colorimetric biosensors are highlighted, aiming at improving the overall performance from different approaches.

[a]*Department of Biomedical Engineering, Shenzhen University Medicine School, Shenzhen University, Shenzhen, 518055, China. E-mail: 2194311415@qq.com, 310165652@qq.com, hangjiaovo@gmail.com, chaiyj@szu.edu.cn, chenww@szu.edu.cn*
[b]*College of Materials Science and Engineering, Shenzhen University, Shenzhen, 518055, China. E-mail: 15220204736@163.com*

1. Introduction

Exosomes are small extracellular vesicles (EVs) formed within multivesicular bodies in the endosomal system of various cell types, playing important roles in cell-to-cell communication and various physiological or pathological processes.[1–3] Since the surface and internal cargos are highly variable and resemble their cells of origin, exosomes have drawn great

Zhonghao Sun is an undergraduate student in the Department of Biomedical Engineering at Shenzhen University. His research interests include the development of colorimetric biosensors for exosomes.

Zhonghao Sun

Binmao Zhang received his B.E. degree in Guangdong Medical University in 2022. He is a master's degree candidate in the Department of Biomedical Engineering at Shenzhen University. His research interests include whole blood manipulation and chemiluminescence immunoassays.

Binmao Zhang

attention in the field of disease detection and therapeutics, particularly as the target for non-invasive early diagnosis.[4–6]

Exosomes exist in all types of body fluids, including blood, saliva, urine, and breast milk.[7] Significantly higher blood exosome concentrations have been reported in cancer patients compared with healthy individuals, correlated with the active reprogramming, rapid growth, and metastasis of tumor cells.[8–11] For patients with Alzheimer's disease, higher levels of Aβ42 and tau proteins were found in neuron-derived exosomes, associated with the level of disease progression.[12,13] Thus, accurate, sensitive, and convenient quantification of exosomes is the first step towards downstream investigations and holds immense potential in clinical applications of various fields.[14,15]

Several methods have been developed to quantify exosomes, including nanoparticle tracking analysis (NTA), dynamic light scattering (DLS), transmission electron microscopy (TEM), flow cytometry, and immunoassays.[16,17] NTA and DLS provide information about the size and concentration of exosomes using light scattering techniques.[18] The former was intensively used as the reference method for exosome biosensor development, generating a quantitative result for the particle concentration of the sample. TEM is commonly employed for the visual characterization of exosomes, allowing for size determination and the estimation of quantity.[19] However, these methods involve the operation of complicated machines and mostly rely on the physical properties of exosomes. Precise quantification of exosomes could also be achieved through a biochemical approach based on immunological recognition between antibodies/aptamers and exosome tetraspanin proteins such as CD63, CD9, and CD81.[20,21] Immunoassays such as enzyme-linked immunosorbent assay (ELISA) and lateral-flow immunoassay (LFIA) demonstrate advantages in the operation procedure, specificity, and cost, which are frequently used in exosome analysis.

Among the immunoassays, enzyme-based colorimetric biosensors are particularly important due to their signal generation and collection method, especially visible colorimetric detection whose readout is based on absorption. The enzymes catalyze transparent substrates such as 3,3′,5,5′-tetramethyl benzidine (TMB) into colorimetric molecules, offering visible results and convenient diagnosis with minimal requirement of devices.[22] However, traditional colorimetric biosensors of exosomes face numerous challenges, including a narrow detection range, unsatisfactory sensitivity, and a long reaction time. Great efforts have been made in the past few decades to explore novel enzymes with higher efficiency and reaction design that can enhance the performance of colorimetric assays.[23] Encouragingly, materials with enzyme-mimetic properties known as nanozymes emerged in 2007.[24] Soon after, various types of nanozymes including gold nanoparticles (AuNPs), carbon nanomaterials, DNAzyme nanomaterials, magnetic nanomaterials, and metal–organic frameworks (MOFs) have been applied as exosome colorimetric biosensors.[25,26] The robust physical and chemical properties of these nanozymes make them promising candidates as enzymatic counterparts.[27] Additionally, the design of assays with nanozymes demonstrated a diverged path from the ongoing studies using natural enzymes, both leading to the rapid progression of exosome research toward clinical applications.[26,28]

In recent years, several comprehensive reviews have been published regarding the detection of exosomes. Zhu *et al.* summarized the advances of single-stranded DNA (ssDNA) aptamer-based sensors for cancer and tumor-derived exosomes.[29] Zheng *et al.* presented the achievements of lipid anchor-based biosensors for the isolation and detection of exosomes and made comparisons between different types of probes.[30] Xiong *et al.* conducted a systematic review of various detection methods for cancer-derived exosomes, offering a comprehensive overview of different strategies and evaluating their analytical performance.[31] However, to our knowledge, the application of natural enzymes and nanozymes in exosome colorimetric biosensors has not been elaborated. With the accumulation of novel components, designs, and remarkable improvements in biosensor performance, it is necessary to summarize and discuss the advances in this specific field and make a comparison of the novel strategies from the perspective of catalytic materials.

This review aims to provide a comprehensive overview of recent advancements in enzyme-based colorimetric detection

Hangjia Tu received her Bioengineering degree from Zhejiang University of Science and Technology in 2023. She is a master's degree candidate in the Department of Biomedical Engineering at Shenzhen University. Her research interests include digital microfluidics.

Hangjia Tu

Chuye Pan is currently an undergraduate student at the College of Materials Science and Engineering at Shenzhen University. His research interests include functionalized nanocomposites and catalytic technologies.

Chuye Pan

methods for exosomes. Many of these technologies enabled the measurement of exosome particle concentration, which is particularly crucial in non-invasive early diagnosis of various types of diseases. First, the principles and mechanisms of colorimetric assays for exosomes will be introduced. Then, relevant studies will be categorized into two main sections based on the types of enzymes utilized: natural enzymes and nanozymes. An in-depth discussion of the biosensor design and performance will be provided, based on the properties of the catalytic materials. To underscore the significance of nanozymes in exosome detection, a comparison is made between the properties and methodologies of natural enzymes and nanozymes. Finally, the advantages and challenges of nanozyme-based exosome isolation and colorimetric detection are presented, emphasizing their great potential in future research and commercialization.

2. Principles and mechanisms of enzyme-based colorimetric assays

In this review, the colorimetric detection of exosomes will be introduced and discussed from the aspects of natural enzyme-based and nanozyme-based reactions. Both enzymes harbor the catalytic activity (mainly peroxidase or oxidase) to boost the colorimetric signal for visual assessment. However, the design of biosensors and the operation procedures were quite different, depending on the unique properties of enzymes and the detection platforms (Fig. 1).

2.1 Natural enzyme-based assays

The general principle of natural enzyme-based immunoassays for exosomes is quite mature and adopted by commercialized detection kits. Horseradish peroxidase (HRP) and alkaline phosphatase (ALP) are the most widely used natural enzymes for diagnosis, as they catalyze colorless substrates such as TMB, 2,2′-azino-bis(3-ethylbenzothiazoline-6-sulfonic acid) (ABTS) and dopamine (DA) for the generation of colorimetric signals.[32,33] Both HRP and ALP reach their optimal activity at around 25–37 °C, exhibiting limited stability at high temperatures over 40 °C.[32] Compared with Fe_3O_4-based nanozymes, HRP required a much lower H_2O_2 concentration (less than 1/5) to reach the desirable peroxidase activity.[24]

Colorimetric exosome biosensors based on natural enzymes often adopt a typical sandwich-like structure, amplifying the detection signal that is proportional to the concentration of exosomes (Fig. 1A). Various platforms or materials have been developed during the past decades, including paper-based analytical devices (PADs), microbead-based isolation and detection techniques, and microfluidic systems.[34–36] Specific capture agents such as antibodies and aptamers, or nonspecific capture agents such as lipid anchors can be immobilized on these materials for selective binding and isolation of exosomes. Natural enzymes are often modified on detection probes including detection antibodies, aptamers, or lipid anchors to catalyze the colorimetric signals. The sensitivity of assays can be achieved through enzymes or specially designed detection probes with amplification potential.[9,35,37]

2.2 Nanozyme-based assays

Nanomaterials with unexpected enzyme mimics have drawn great attention and achieved considerable advances in biomedical applications due to the tremendous progress in nanotechnology and their unique characteristics.[38–40] They can be categorized based on the type of enzymatic activity (peroxidase, catalase, oxidase, superoxide dismutase, hydrolase), or the composition of materials that determined their enzymatic properties and operation principles.[41–43] In this review of

Yujuan Chai, Ph.D. is an assistant professor at the Department of Biomedical Engineering, School of Medicine, Shenzhen University. She received her Ph.D. degree from the School of Public Health, Li Ka Shing Faculty of Medicine, the University of Hong Kong in 2016, and her B.S. degree from the Department of Biochemistry and Biomedical Science, McMaster University in 2012. With 23 publications and 4 years of working experience as an R&D scientist in the in vitro *diagnostics industry, her field of interest includes immunoassay-based biosensors, synthesis and characterization of fluorescent nanoparticles, and microfluidic chip-based bioassays.*

Yujuan Chai

Wenwen Chen, Ph.D. is an associate professor at the Department of Biomedical Engineering, School of Medicine, Shenzhen University. She obtained her B.Sc. degree from China Agricultural University (2010), followed by a Ph.D. (2015) from the National Center for Nanoscience and Technology, Chinese Academy of Sciences. She joined Shenzhen University Health Science Center as a lecturer in 2015. From June 2019 to June 2020, she was a visiting scholar at Harvard University. Since 2020, she has been an associate professor (PI) at Shenzhen University. Her main research interests are focused on the development of advanced diagnostic and therapy methods based on microfluidics and nanotechnology.
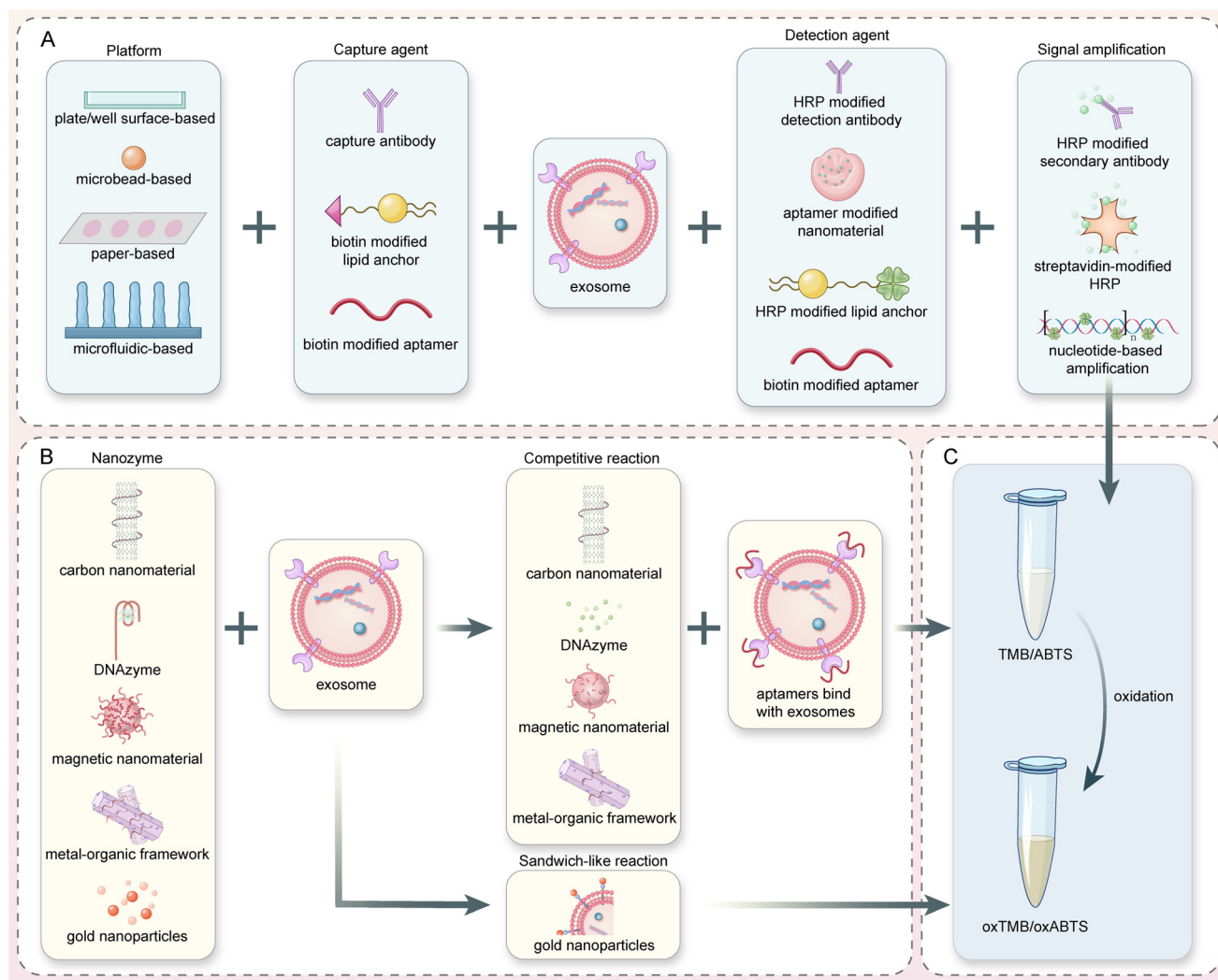
Wenwen Chen

Fig. 1 General principles of natural enzymes and nanozyme-based colorimetric biosensors for exosomes. (A) Schematic of the sandwich-structured reaction in natural enzyme-based assays. (B) Schematic of the competitive reaction in nanozyme-based assays. (C) Colorimetric reactions catalyzed by natural enzymes or nanozymes using TMB or ABTS as substrates.

exosome colorimetric biosensors, the function and properties of 5 types of nanozymes will be explored (gold nanoparticles, carbon nanomaterials, DNAzymes, magnetic nanomaterials, and metal–organic frameworks).

The effectiveness of nanozymes varies for a broad range depending on their instinct properties such as structure, composition, and shape, but also acquired surface functionalization.[44–46] For instance, the peroxidase activity of Fe_3O_4 nanoparticles demonstrated a 10-fold enhancement upon the surface absorption of DNA.[47] Thus, the design of nanozyme-based biosensors is typically based on the manipulation of their catalytic ability through reversible surface modification with nucleotides or amino acids that could specifically interact with target exosomes.[25,48] When a competitive assay design was adopted, aptamers of exosome surface proteins were firstly capped on the nanozymes, boosting the peroxidation or oxidation efficiencies. During sample incubation, the

aptamers will relocate to the exosome surface due to higher immunoaffinity to the biomarkers. In this way, the exosome concentration can be translated into the change of nanozyme activity through a single step, resulting in a noticeable change in colorimetric reactions (Fig. 1B). Therefore, with the same types of substrates (TMB, ABTS, and H_2O_2), nanozyme-based exosome biosensors generally require fewer operations, bioreagents, and reaction time.

3. Natural enzyme-based colorimetric detection of exosomes

In recent years, natural enzyme-based colorimetric exosome biosensors coupled with novel signal amplification techniques and reaction designs have achieved an improved level of sensitivity to meet the requirements of laboratory and clinical experiments.

More importantly, the enzymes and basic reaction principles have been integrated into various platforms, such as paper-based analytical devices, microbeads, and microfluidic-based platforms, further enhancing the test performance from different aspects such as efficiency, convenience, and sample consumption. Since the type of natural enzyme utilized in exosome biosensors was limited (HRP and ALP only), the comprehensive discussion of these analytical techniques in the following subsections was categorized according to the platforms employed. A detailed summarization of the natural enzyme-based colorimetric biosensors is presented in Table 1.

3.1 Enzymes linked immunosorbent assays

Enzyme-linked immunosorbent assay (ELISA) with a 96-well plate is widely used in research and clinical applications as a relatively mature analytical tool for the quantification of protein biomarkers.[22] ELISA is often used to detect the particle concentration of exosomes or differentiate tumor cell-derived exosomes from normal ones.[37,49,50] HRP and ALP are commonly used in ELISA to catalyze the colorimetric signals. In most cases, these enzymes will be anchored to the detection probes targeting exosome proteins through streptavidin–biotin interaction. In a special design, the ALP enzymes naturally expressed on the syncytiotrophoblast extracellular vesicles (STBEV) can be used directly for substrate oxidation.[51] This innovative design based on the characteristics and placental origin of the STBEV provides insight into the development of biosensors without the external enzymes typically employed.

In the past decade, efforts have been made to integrate novel binding or signal amplification methods into the classical ELISA-based exosome detection methods. For example, a cactus-inspired dual-modal biosensor has been developed with cholesterol-based-HRP anchors (Fig. 2A). With the highly efficient, nonspecific insertion of the lipid anchors into the exosome membrane, an "one to many" signal amplification process occurred. A limit of detection (LOD) of 3.40×10^3 par per µL and a linear range (LR) from 1.0×10^4 to 5.0×10^5 par per µL were achieved for this colorimetric assay.[50] In another study, the quantification of colorectal cancer (CRC) exosomes was realized through the terminal deoxynucleotidyl transferase (TdT)-aided ultraviolet signal amplification method (Fig. 2B).[37] After the exosomes were captured by A33 antibodies on a 96-well plate, EpCAM aptamer–Au-primer complex was added and extended with poly biotin-adenine chains with the assistance of TdT. The number of avidin-linked HRP can be boosted to achieve a highly sensitive colorimetric detection of exosome (LOD of 6.7×10^3 par per µL, LR of 9.75×10^3–1.95×10^6 par per µL). As one of the most robust and mature methods, ELISA was widely used for both research and clinical applications. However, it is worth noting that the traditional ELISA method for colorimetric exosome detection requires multistep manual operation and long reaction times.

3.2 Paper-based colorimetric immunoassays

Paper-based analytical devices (PADs) based on chromatography are commonly used for point-of-care testing (POCT) due to their rapid reaction and ease of use.[52,53] In a paper-based enzyme-linked immunosorbent assay (P-ELISA), exosomes were captured by antibodies immobilized in the test zone and detected by anti-CD9 primary antibody and HRP-linked secondary antibody.[54] After the substrate was added, the blue precipitants that appeared on these test zones could be scanned with a desktop scanner for signals. With only 10 µl of the sample, this colorimetric reaction can be finished within 10 minutes Recently, Lai et al. developed a paper-based immunoaffinity device and a paper-based silica device for the isolation and quantification of exosomes and exosomal nucleic acids, respectively.[34] The former was employed to capture the concentrated exosomes and carry out the HRP-based colorimetric quantification of particles (0.98×10^5–9.5×10^5 par per µL). Since the purpose of this system was to determine the concentration of exosomal microRNA 21, the captured exosomes were then lysed and the nucleic acids were absorbed by the paper-based silica devices for reverse transcription-quantitative polymerase chain reaction (RT-qPCR).

These studies highlight the low sample volume required by paper-based exosome detection and the reduction of cost for the consumables. Paper-based immunoaffinity devices exhibit immense potential for POCT applications, particularly in resource-limited areas.

3.3 Microbead-based immunoaffinity detection of exosomes

Microbeads, such as magnetic beads (MBs), latex beads (LBs), and silica beads (SBs), are common tools of exosome biosensors, enabling a large-area 3D stationary phase for highly efficient antibody conjugation and exosome capture compared with the traditional 2D reaction in ELISA.[55] MBs consist of a core material, frequently composed of iron oxide or other magnetic substances, and enveloped by a surface layer or shell that can be modified for specific applications. LBs and SBs are fabricated from a variety of polymers such as polystyrene, polyethylene, or silica.

Compared with the conventional design of magnetic beads (MBs) biosensors, new strategies incorporating lipid anchors for exosome binding have been developed in the past decade.[8,56–58] Due to the hydrophobic interaction, amphiphilic lipid molecules such as modified C18, cholesterol, and 1,2-distearoyl-sn-glycero-3-phosphoethanolamine (DSPE) can be inserted into the exosome membrane automatically to achieve the isolation or detection of exosomes.[59] An innovative design combined cholesterol-modified MBs for exosome capture and horseradish peroxidase-encapsulated DNA nanoflowers (HRP-DFs) as detection probes (Fig. 2C).[8] Quantitative detection of exosomes was achieved through the HRP-DFs catalyzed oxidation of ABTS, generating colorimetric and absorbance signals that could be detected by UV-vis spectroscopy. It is noteworthy that HRP-DFs demonstrate better catalytic activity and biological stability compared to conventional HRP-labeled ssDNA. Taking advantage of the superior performance of HRP-DFs, a linear range from 5.0×10^3 to 5.0×10^6 par per µL with a low LOD of 3.32×10^3 par per µL was achieved.

Table 1 Summarization of natural enzyme-based colorimetric exosome biosensors

Category	Catalyst	Chromogenic system	Time (min)	Performance (par per µL)	Advantages	Limitations	Ref.
ELISA	ALP	NADPH	180	NA^a (quantified through flow cytometry) (relative numbers only)	Utilize membranous human placental alkaline phosphatase and specific detection of preeclampsia-specific EVs	Variations in phosphatidylserine availability on the exosome surface; Interference from other phosphatase-carrying EVs	51
	HRP	PPD–H$_2$O$_2$	220	LOD: 3.40×10^3 (UV-vis), LOD: 3.12×10^3 (Fluor) LR: 1.0×10^4–5.0×10^5, LOD: 6.7×10^3	Dual-modal biosensor	Narrow detection range	50
	HRP	TMB–H$_2$O$_2$	220	LR: 9.75×10^3–1.95×10^6	Highly efficient lipid anchor-based probes	Time-consuming; Temperature control for the whole reaction	37
Paper-based	HRP	TMB–H$_2$O$_2$	10	NA	TdT-based signal amplification; Distinguish clinical samples; Rapid	LOD and LR of exosomes not specified; Complicated operation steps	54
	HRP	TMB–H$_2$O$_2$	120	NA (quantify miRNA)	Promising for POCT; Easy operation for exosome extraction	LOD and LR of exosomes not specified	34
Microbead-based	HRP	TMB–H$_2$O$_2$	980	LOD: 2.2×10^3 LR: 2.3×10^3–2.3×10^5	Promising for POCT; Sensitive; High reproducibility	Time-consuming; Fresh preparation of probes	35
	HRP	DA–H$_2$O$_2$	290	LOD: 7.7 LR: 7.7–10^7	Extremely sensitive and wide detection range; Multi-step signal amplification	Fresh preparation of DA solution; Complicated operation steps and long-time	61
	HRP	ABTS–H$_2$O$_2$	65	LOD: 3.32×10^3 LR: 5×10^3–5×10^6	DNA flower-based biorecognition; Multi-step signal amplification	Multiple types of enzymes required	8
	HRP	TMB–H$_2$O$_2$	150	LOD: 10^2 LR: 2×10^2–10^3	Dual signal amplification through RCA; High sensitivity	Narrow detection range	9
Microfluidic-based	HRP	TMB–H$_2$O$_2$	170	LOD: 2.76×10^3; LR: 2.76×10^3–4.15×10^4	Sensitivity	Complicated fabrication of the device and pump required; Narrow detection range	62
	HRP	TMB–H$_2$O$_2$	130	LOD: 35.0×10^{-3} AU per µl^a; LR: 10^{-1}–10^3 AU per µl^a	Detect multiple biomarkers; Size-exclusion membrane-based EV isolation	Temperature control for multiple steps; Pump required; Arbitrary unit used	63
	HRP	TMB–H$_2$O$_2$	60	LOD: NA; LR: NA	Smart phone-assisted imaging; Rapid, size-selective spinning disc for EV isolation; >95% recovery rates	LOD and LR not specified	64
	HRP	TMB–H$_2$O$_2$	135	LOD: 2.2×10^4	Improved capture efficiency with ZnO nanowire 3D scaffold device; Reaction at room temperature	Less sensitive	36
	HRP	TMB–H$_2$O$_2$	90	LR: 2.2×10^5–2.4×10^7 LOD: NA; LR: 2–16 AU per µl^a	Streamlined on-chip procedure; Optimized observation chamber height	Pump needed; Pump required; Arbitrary unit used	65
pH-Responsive	HRP/urease	Phenol red–urea	245	LOD: 4.46×10^3 LR: 5×10^3–1×10^6	pH test paper-based signal readout; No need for expensive instruments	Time-consuming; Multiple types of enzymes required	10
	AChE	Phenol red–Ach	60	LOD: 1.2×10^3 LR: 2.0×10^3–5.0×10^5	Obvious color change in the dynamic range; High consistency and recovery rate	Complicated fabrication of DNA microcapsules	11

Abbreviations: LOD: limit of detection; LR: linear range; NA: not available; ELISA: enzyme linked immunosorbent assay; ALP: alkaline phosphatase; NADPH: nicotinamide adenine dinucleotide phosphate HRP: horseradish peroxidase; PPD: 1,4-phenylenediamine; TMB: 3,3′,5,5′-tetramethylbenzidin; ABTS: 2,2′-azino-bis(3-ethylbenzothiazoline-6-sulfonic acid); EV: extracellular vesicle; TdT: terminal deoxynucleotidyl transferase; POCT: point-of-care testing; UV-vis: ultraviolet-visible spectroscopy; Fluo: fluorescence; DA: dopamine; RCA: rolling circle amplification; AU: arbitrary unit; and AChE: acetylcholinesterase; the reaction time is estimated based on the protocol described in the Methods section of each study if a total time is not mentioned. ^{a} Arbitrary unit was used instead of NTA-based quantification of the particle number.
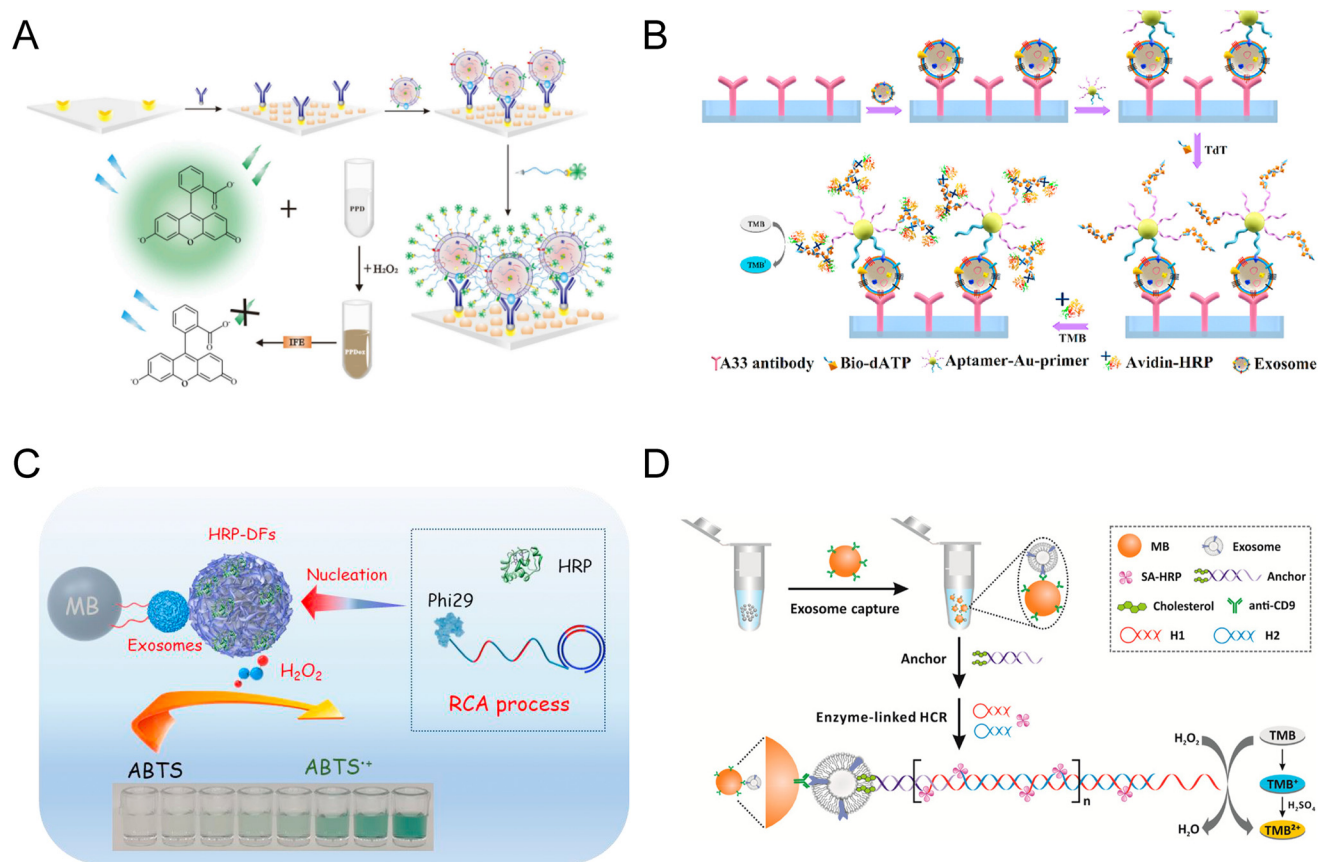
Fig. 2 Microplate and microbead-based colorimetric exosome detection. (A) A nature-inspired dual-model biosensor using a monovalent cholesterol probe consisting of ssDNA and HRP. Reproduced from ref. 50 with permission from Elsevier, copyright 2020. (B) A biosensor for colorectal cancer exosomes that utilizes a TdT-facilitated signal amplification system. Numerous avidin-HRP molecules can bind to the extended DNA chain, catalyzing a colorimetric assay. Reproduced from ref. 37 with permission from Elsevier, copyright 2020. (C) An innovative colorimetric biosensor that integrated HRP-encapsulated DNA nanoflowers as the detection probe and signaling tag. The nanoflowers were synthesized by rolling circle amplification (RCA) and can subsequently catalyze the ABTS–H$_2$O$_2$ color-changing system. Reproduced from ref. 8 with permission from Elsevier, copyright 2021. (D) Reaction principle of a BC anchor-based exosome biosensor. Primary signal amplification is achieved through HCR, which is initiated by BC-labeled DNA trigger sequences and H1 and H2 probes. Secondary signal amplification and colorimetric signals are generated through SA-HRP or SA-ALP enzymes attached to the biotins on H1 and H2. Reproduced from ref. 35 with permission from the American Chemical Society, copyright 2017.

An alternative approach is to combine the MB capture agent with detection probes/natural enzymes that are linked with lipid anchors. In the study of He *et al.*, anti-CD9 antibody-coated MBs were used for exosome isolation from human serum samples (Fig. 2D). Afterward, bivalent-cholesterol anchors with complementary ssDNA anchored to the exosomes spontaneously, forming dsDNA with sticky ends that could initiate the hybridization chain reaction (HCR). During HCR, a long-nicked chain structure made of numerous HRP-labeled DNA hairpins would form, catalyzing the colorimetric signals for exosome quantification. The system could reach a 100-fold higher sensitivity (LOD of 2.2×10^3 par per μL) with a linear range of 2.3×10^3–2.3×10^5 par per μL.[35] In a recent study, a dual signal amplification biosensor was constructed for the visual detection of leukemia exosomes.[9] Initially, the aptamers of the nucleolin biomarkers were hybridized with the trigger probes functionalized on the MBs, inhibiting the rolling circle amplification (RCA).[60] Capturing of exosomes with aptamers led to the release of trigger probes from the MBs, which can further hybridize with padlock probes of the RCA reaction. The numerous repeated sequences generated through RCA would bind to many short signal probes labeled with biotin. Finally, the HRP-modified gold nanoparticles (GNPs-HRP) bound to the signal probes through streptavidin–biotin reaction and catalyzed the colorimetric reaction. This colorimetric biosensor utilizing RCA and GNPs-HRP dual amplification method exhibited outstanding LOD as low as 100 par per μL.

LBs with special surface modification were also employed as capture agents in the colorimetric detection of exosomes. In an ExoAptaSensor reported by Xu *et al.*, exosomes were captured directly by latex beads through non-specific aldimine condensation. Subsequently, CD63 aptamers with HRP were applied, catalyzing the colorless dopamine (DA) to the brown-black polydopamine (PDA) around the exosome particles. This *in situ* reaction enhanced the sensitivity of the colorimetric biosensor to an impressive LOD as low as 7.7 par per μL,

which is around 3 orders of magnitude compared with traditional immunoassays.[61]

Microbeads serve as fundamental components in a wide range of clinical assays and commercialized platforms because they offer a notable advantage in sample concentration compared to microplates and paper-based platforms. It can capture and concentrate large volumes of exosomes through magnetic force or centrifugation, leading to a significant enhancement in the sensitivity of colorimetric reactions. While microbeads are valued for their biocompatibility and versatility, the capture time for exosomes is usually long and the nonspecific binding should be noticed. Researchers are aiming at mitigating these drawbacks and enhancing the overall efficiency of microbead-based exosome biosensors.

3.4 Microfluidic-based colorimetric immunoassays

Microfluidics as powerful tools have been developed for a wide range of biomedical applications, including the colorimetric detection of exosomes. In 2014, a multiplexed microfluidic platform based on an alternating current (AC) electrohydrodynamic (ac-EHD) induced surface shear force was constructed (Fig. 3A).[62] This AC-EHD-induced nano-shearing microfluidic device can increase the number of exosome-antibody collisions, thus enhancing the specific binding between exosomes and antibodies. The device offers a simple and rapid on-chip naked eye detection readout based on the colorimetric reaction between HRP and TMB. Due to the microenvironment and nano shearing, the device exhibited a 3-fold enhancement in detection sensitivity in comparison to hydrodynamic flow-based assays, reaching a LOD of 2.76×10^3 par per µL and a linear range of 2.76×10^3–4.15×10^4 par per µL.[62]

Moreover, microfluidic systems exhibit the dual capability of exosome isolation and detection. In the studies conducted by Woo et al. and Liang et al., the isolation of nanoscale extracellular vesicles based on multilayer size-exclusion microfluidic chips was achieved with high efficiency.[63,64] Subsequently, on-chip ELISA for the quantification of specific transmembrane proteins was realized. Chen et al. reported a microfluidic system that enables on-chip immune isolation and in situ protein analysis of exosomes with the integration of MBs and
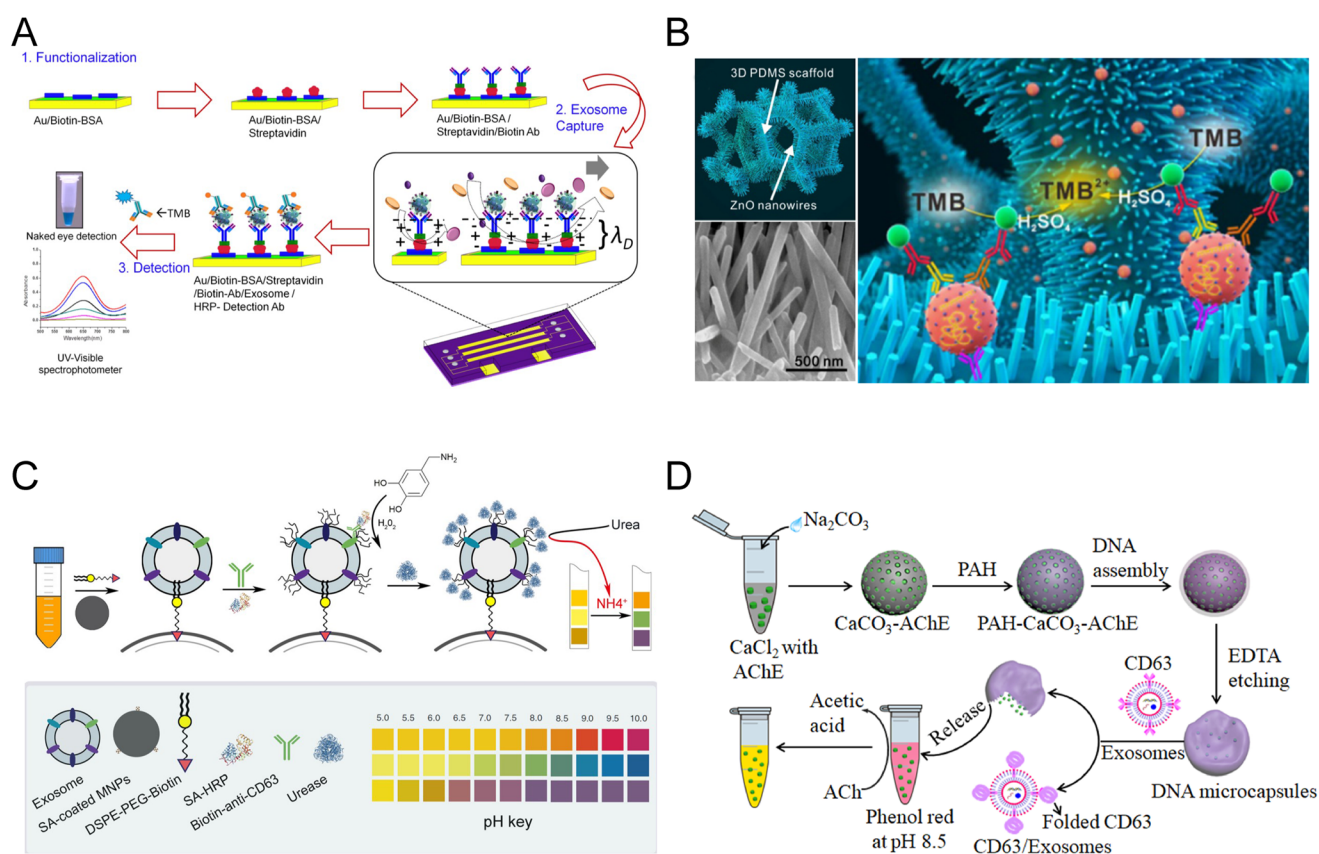

Fig. 3 Schematics of microfluidic-based and pH-responsive colorimetric biosensors of exosomes. (A) Microfluidic platform embedded with an AC-EHD-induced surface shear force for exosome detection. Reproduced from ref. 62 with permission from the American Chemical Society, copyright 2014. (B) A ZnO nanowire-coated 3D microporous chip for efficient isolation and colorimetric quantification of exosomes. Reproduced from ref. 36 with permission from Elsevier, copyright 2018. (C) Schematic of the pH-responsive assay for colorimetric quantification of exosomes. The biotin of the DSPE lipid anchor exposed on the exosome surface enabled the attachment of SA-HRP and urease, triggering the increase of pH with enzymatic reaction. Reproduced from ref. 10 with permission from Elsevier, copyright 2019. (D) Another pH-sensitive colorimetric biosensor using aptamer DNA microcapsules containing AChE. The binding of exosome CD63 with aptamers leads to the release of AChE and the catalysis of substrates. Reproduced from ref. 11 with permission from Elsevier, copyright 2022.

3-layer microstructures.[65] The reaction was driven by programmable micropumps and microvalves, resulting in a shorter reaction time (~1.5 h) and a high enrichment efficiency of 74.17%. The performance of microfluidic-based colorimetric exosome assays can be further improved by the incorporation of other nanomaterials and nanostructures.[66] For instance, a zinc oxide (ZnO) nanowires-coated 3D macroporous chip (ZnO-chip device) has been applied to the efficient isolation and colorimetric quantification of exosomes (Fig. 3B).[36] With a simple microfluidic channel, the hierarchical nanointerface provided by the ZnO nanowires that grow on the surface of a 3D scaffold formed a nanowire forest, increasing the surface area for affinity capture of exosomes. This nanostructure also provides an exclusion-like effect with the nanowires of exosome-size spacing, further improving the capture efficiency. After the capture of exosomes on nanowires, immunoaffinity assays similar to ELISA were conducted. The ZnO-chip device enabled the isolation and detection of exosomes from 100 μl serum samples within 2.5 h, with an LOD of 2.2×10^4 par per μL and a linear range of 2.2×10^5–2.4×10^7 par per μL.

The integration of microfluidic devices into exosome analysis offers advantages such as reduced analysis cost, decreased reagent volume, a high surface-to-volume ratio for immunoaffinity interactions, and simplified handling.[66,67] The incorporation of nanomaterials into the microfluidic device introduced complicated structures and microenvironments to enhance the reaction efficiency for both the antibody and exosomes and the enzyme and substrates.[36,62]

3.5 pH-Responsive immunoaffinity detection of exosomes

In addition to the aforementioned strategies, biosensors of exosomes also involve colorimetric reactions that translate the quantity of exosomes into the change in pH values.[10,11] The first pH-responsive biosensor was used in conjugate with lipid anchor-coated MBs (Fig. 3C). After the exosomes were captured through hydrophobic interaction, CD63 antibodies coupled with HRP rapidly catalyzed the deposition of PDA on exosome surfaces. Through PDA film, urease can be immobilized on exosomes and automatically hydrolyze urea into ammonia and carbon dioxide, raising the pH of the solution. With this method, a limit of detection (LOD) of 4.46×10^3 par per μL and a detection range of 5×10^3–1×10^6 par per μL were achieved.[10] Another recently developed pH-sensitive exosome biosensor was proposed by Shen *et al.*, where a novel acetylcholinesterase (AChE) loaded DNA microcapsule was synthesized (Fig. 3D). The shell of the microcapsules was composed of anti-CD63 aptamers, which will dissociate upon the recognition of CD63 proteins on the surface of exosomes. The encapsulated AChE was then released, hydrolyzing acetylcholine (Ach) to acetic acid in the presence of phenol red indicator, converting the concentration of exosomes into the color change and the alteration of the pH value. This method allows the quantitation of exosomes between 2.0×10^3 par per μL and 5.0×10^5 par per μL, with an LOD of 1.2×10^3 par per μL.[11]

These pH-responsive immunoaffinity detection methods rely on colorimetric signals and changes in pH values, which can also be quantified using pH test strips. The pH test strips are often more accurate than visual observations, making a reliable readout when UV-visible spectroscopy is not available. Compared with the aforementioned colorimetric exosome tests, the pH-responsive colorimetric assays hold promise for clinical diagnosis in underprivileged and remote areas lacking expensive instruments.

4. Nanozyme-based colorimetric detection of exosomes

Though widely applied in various colorimetric assays, natural enzymes suffer from intrinsic limitations such as low stability, difficulties in production, and high cost. Therefore, nanozymes, nanomaterial-based artificial enzymes, emerged and acquired increasing popularity in the development of colorimetric assays for exosomes due to their unique catalytic properties and reaction mechanisms.[48]

Nanomaterials with inherent enzyme mimetic properties were characterized by Gao *et al.* early in 2007, showing that the Fe_3O_4 magnetic nanoparticles (Fe_3O_4-MNPs) exhibit similar activity and superior stability compared to conventional HRP.[24] Since then, a cascade of nanozymes possessing remarkable enzyme-like activities has been discovered and used in biomedical assays, fulfilling the capture, isolation, and detection function in the biosensors. These nanozymes possess advantages such as enhanced stability, durability, and low cost, which are particularly beneficial for various biomedical applications.[68] One of the most important features of many nanozymes is the adsorption of exposed nucleobases of single-stranded DNA (ssDNA) through van der Waals forces. For double-stranded DNA (dsDNA), however, the absorption between embedded nucleobases and nanomaterials is much weaker.[69] This selective absorbance enabled the modification of nanozyme activity through competitive binding of the ssDNA (aptamers in most cases), translating the target protein or exosome concentration to a colorimetric readout.[70] Due to the difference in size and binding kinetics between free protein biomarkers and exosomes, the specific recognition and nonspecific recognition of target molecules embedded in exosome membranes were generally slower. Point-of-care-testing of free protein targets was quite common, but relatively rare for exosomes. The application of nanozymes and the adoption of competitive assay design significantly reduced the reaction time of exosome biosensors and improved the applicabilities.

Different from the HRP-based assays that are conducted on various types of platforms, nanozyme-based colorimetric biosensors are mostly performed in test tubes. They are typically designed based on the unique biochemical properties and categories of the nanozymes. Therefore, the following detailed discussion of nanozyme-based exosome colorimetric biosensors is categorized according to the types of nanozymes. A summarization of these assays can be found in Table 2.

Table 2 Summarization of nanozyme-based colorimetric exosome biosensors

Category	Catalyst	Chromogenic system	Time (min)	Performance (par per μL)	Advantages	Limitations	Ref.
Carbon nanomaterials	s-SWCNTs	TMB–H_2O_2	40	LOD: 5.2×10^5 LR: 1.84×10^6–2.21×10^7	Convenient, rapid, and cost-efficient system Potential for POCT	Less sensitive Narrow linear range	73
	g-C_3N_4 NSs	TMB–H_2O_2	30	LOD: 13.52×10^5 LR: 0.19×10^7–3.38×10^7	Convenient, rapid, and cost-efficient system Potential for POCT	Less sensitive Narrow linear range	74
DNAzymes	Hemin/G-quadruplex	ABTS–H_2O_2	140	LOD: 3.94×10^2 LR: 8.3×10^2–5.3×10^4	Convenient, sensitive, and cost-efficient system Label-free detection	Pre-isolation with MBs required	82
	Hemin/G-quadruplex	TMB–H_2O_2	60	LOD: 3.94×10^2 LR: 10^3–10^5	Convenient and time-saving Effective in serum samples	Temperature control needed	86
	Aptamer/split DNAzyme complex	ABTS–H_2O_2	210	LOD: 1 LR: 1.0×10^3–1.0×10^7	Highly sensitive with broad LR Dual-modal biosensors	Temperature control for multiple steps	87
Magnetic nanomaterials	Fe_3O_NPs	TMB–H_2O_2	30	LOD: 3.58×10^3 LR: 0.4×10^5–6.0×10^5	Labeling-free, rapid, and cost-efficient system Convenient anion exchange-based isolation	Narrow LR Non-specific isolation required exosome elution	90
	Au-NPFe_2O_3NC	TMB–H_2O_2	140	LOD: 1 LR: 1–10^4	Highly sensitive with broad LR Free of pre-isolation	Special screen-printed carbon electrode surface required	91
	Fe_3O_4–Cu^{2+}–NZs	TMB–H_2O_2	131	LOD: 5.91×10^3 LR: 1.4×10^4–5.6×10^5	Labeling-free detection without pre-isolation Effective in serum samples	Temperature control for multiple steps	92
Metal-organic frameworks	$CuCo_2O_4$ nanorods	TMB	131	LOD: 4.5×10^3 LR: 5.6×10^4–8.9×10^5	Labeling-free detection without pre-isolation Effective in serum samples	Temperature control for multiple steps Narrow LR	98
	Fe-MOFs	TMB–H_2O_2	17	LOD: 5.2×10^4 LR: 1.1×10^5–2.2×10^7	Very fast, labeling-free cost-efficient system Effective in serum samples	Less sensitive Temperature control for multiple steps	99
Gold nanoparticles	AuNPs	TMB–H_2O_2	95	LOD: 0.2 ng L^{-1} ^{a} LR: 0.3–200 ng L^{-1}	Low sample volume No preconcentration needed	Temperature control for multiple steps	103
	AuNPs	TMB–H_2O_2	<180	LOD: NA^a LR: 1.375×10^7–2.2×10^8 ng L^{-1}	Lipid anchor-based exosome labeling Detection of multiple exosome surface proteins	Narrow LR Temperature control for multiple steps	104

Abbreviations: LOD: limit of detection; LR: linear range; NA: not available; TMB: 3,3′,5,5′-tetramethylbenzidine; ABTS: 2,2′-azino-bis(3-ethylbenzothiazoline-6-sulfonic acid); HRP: horseradish peroxidase; POCT: point-of-care testing; s-SWCNTs: soluble single-walled carbon nanotubes; g-C_3N_4 NSs: graphitic carbon nitride nanosheets; Fe_3O_4-NPs: Fe_3O_4 nanoparticles; Au-NPFe_2O_3NCs: gold-loaded ferric oxide nanocubes; Fe_3O_4–Cu^{2+}–NZs: iron oxide–copper ion nanozymes; $CuCo_2O_4$ nanorods: Cu/Co bimetallic metal–organic frameworks; Fe-MOFs: iron-based metal–organic frameworks; and AuNPs: gold nanoparticles. ^{a} Quantify exosome surface protein.

4.1 Carbon nanomaterials

Carbon nanomaterials with different structures have been widely used in biological research and the fabrication of colorimetric biosensors.[71] Various carbon nanomaterials possess the ability to selectively adsorb single-stranded DNA (ssDNA), altering the peroxidase activity of these materials significantly.[47,72–74] Xia *et al.* proposed an exosome aptasensor integrating soluble single-walled carbon nanotubes (s-SWCNTs), which possess intrinsic peroxidase-like activity for TMB–H_2O_2 (Fig. 4A).[75,76] In the absence of exosomes, CD63 aptamers were absorbed to the surface of s-SWCNTs through noncovalent reactions, thus increasing the peroxidase activity of s-SWCNTs. The competitive binding of aptamers between s-SWCNTs and CD63 protein on target exosomes will release the s-SWCNTs, decreasing the catalytic activity and resulting in a weaker color change. This biosensor reached a LOD of 5.2×10^5 par per μL and a linear range of 1.84×10^6 to 2.21×10^7 par per μL. Although the sensitivity was less satisfactory, the whole

assay took only 40 min, which is much shorter than most exosome detection methods.[73] The study of Wang *et al.* shared a similar idea but replaced the nanotubes with g-C_3N_4 nanosheets (NSs) (Fig. 4B).[74] The absorbance of CD63 aptamers onto the g-C_3N_4 NSs leads to a 4-times acceleration of their catalytic rate compared to the free g-C_3N_4 NSs.[70] In the presence of exosomes, the CD63 aptamers will be released from the NSs and attached to the CD63 with higher affinity. This reduction of NSs peroxidase activity will lead to a weaker blue color of the catalytic products. The detection time of the current assay was shortened to 30 min, achieving a LOD of 13.52×10^5 par per μL and a linear range of 0.19×10^7–3.38×10^7 par per μL. This remarkable biosensor was used to distinguish the exosomes produced by the breast cancer cell line (MCF-7) and control cell line (MCF-10A), exhibiting great potential in clinical settings.

Carbon nanomaterials, either in 2-dimensional (2-D) or 3-dimensional (3-D) forms, offer a high surface-area-to-volume ratio, excellent electrical conductivity, and selective binding
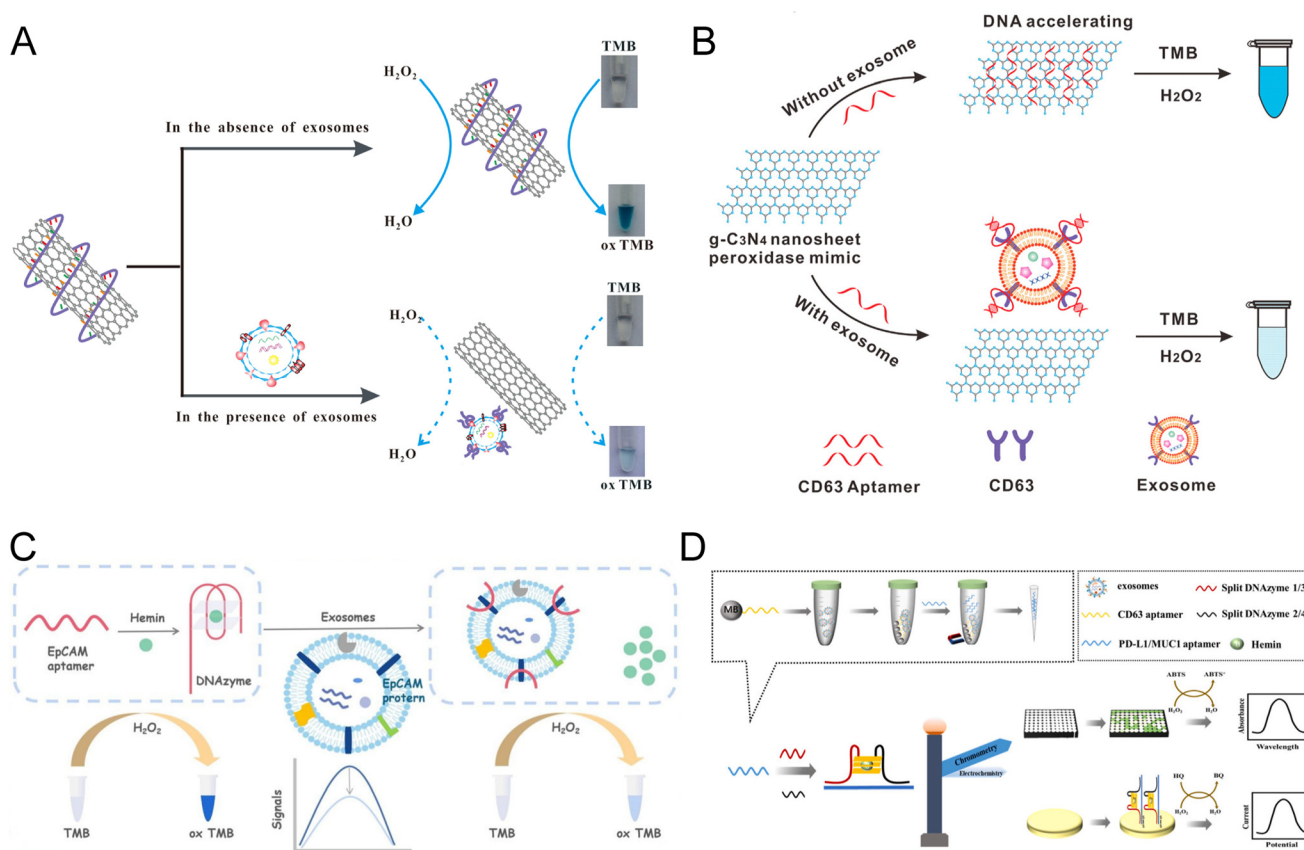

Fig. 4 Colorimetric biosensors constructed with carbon nanomaterials and DNAzymes. (A) Schematic of an s-SWCNT-based competitive assay using CD63 aptamers for the manipulation of nanozyme activity. Translocation of CD63 aptamers from s-SWCNTs to exosome surface proteins decreased the catalytic ability and the color change. Reproduced from ref. 73 with permission from Elsevier, copyright 2017. (B) An aptasensor shared a similar competitive principle but utilized a g-C_3N_4 NS nanomaterial. Reproduced from ref. 74 with permission from the American Chemical Society, copyright 2017. (C) A colorimetric biosensor based on an EpCAM aptamer−DNAzyme probe that can be folded into the G4−hemine DNAzyme structure simultaneously. The nanozyme can be destroyed upon recognition of the exosome EpCAM protein, leading to the reduction of peroxidase activity. Reproduced from ref. 86 with permission from the Royal Society of Chemistry, copyright 2022. (D) Colorimetric biosensor developed based on an asymmetrically split peroxidase DNAzyme. DNAzyme complex was formed by mixing residual aptamers with DNA probes containing split halves of DNAzymes. Reproduced from ref. 87 with permission from Elsevier, copyright 2023.

affinity to ssDNA, enabling the efficient capture and detection of biomarkers. Based on the competitive binding of specific aptamers for exosome proteins, carbon nanomaterials demonstrated a decrease in nanozyme activity, which in turn reflected the target concentration. The simple operation of the competitive assay design enabled a much faster reaction and point-of-care testing for cancer diagnosis.

4.2 DNAzyme nanomaterials

Deoxyribozymes, commonly known as DNAzymes, are single-stranded DNA (ssDNA) molecules capable of catalyzing specific chemical reactions such as nucleotide cleavage, ligation, and peroxidase-mimicking activity.[77–79] Among these, G-quadruplex/hemin (G4–hemin) peroxidase-mimicking DNAzyme (PMD) is one of the most popular materials used in biosensing.[80–83] Facilitated by a hemin cofactor, G4–hemin demonstrates enhanced catalytic activity that can oxidize ABTS (2,2′-azinobis(3-ethylbenzothiazoline-6-sulfonic acid)) or TMB for colorimetric reactions.[84]

Building upon the G4–hemin DNAzyme, Zhou et al. designed a label-free exosome aptasensor with a hairpin probe composed of MUC1 aptamer and mimicking DNAzyme sequence.[85] The specific interaction between the hairpin and exosomal protein triggered the unfolding of the probe and the self-assembly of G-quadruplex subunits into a catalytically active structure. Therefore, the colorimetric signals produced by the DNAzyme are proportional to the concentration of exosomes, and the aptasensor could reach a LOD of 3.94×10^2 par per µL and a linear range of $8.3 \times 10^2 – 5.3 \times 10^4$ par per µL. The current aptasensor strictly controls the process of reaction responding to the existence or not of exosomes, thus being regarded as an "on–off" switch that is highly efficient and sensitive.[82] A modification of the ssDNA aptamer–DNAzyme probe has been in a recent study published by Kuang et al. (Fig. 4C).[86] The aptamer for cancer-related EpCAM protein was adopted due to its abundance of guanine and the ability to form G4–hemine DNAzyme without the introduction of additional sequences. Upon the recognition of exosome EpCAM protein by aptamers, the folded structure of G4–hemine DNAzymes will be destroyed, leading to the reduction of peroxidase activity. A negative correlation between the absorbance and the concentration of exosomes was established within the linear range of $10^3 – 10^5$ par per µL. This 1-hour test was able to analyze cancer cell-derived exosomes in complex biological samples, demonstrating its potential applications in clinical diagnostics. Recently, an innovative dual-modal biosensor based on an asymmetrically split peroxidase DNAzyme has been proposed (Fig. 4D).[87] Different from most aptasensors that utilize the bound aptamer for the generation of detection signals, this assay took PD-L1 or MUC1 aptamers left in the solution as the templates for G4–hemin DNAzyme formation. After incubation with exosomes, free aptamers were separated and mixed with DNA probes containing split halves of DNAzymes with an optimized split configuration of 3 : 1.[88] The resulting DNAzyme complex can be further anchored to a gold electrode, enabling the colorimetric and electrochemical

detection of PD-L1 or MUC1 proteins. This innovative approach reached a remarkably low LOD of 1/0.8 par per µL and a wide linear range of $1.0 \times 10^3 – 1.0 \times 10^7$ par per µL.

DNAzyme nanomaterials, especially the G4–hemin DNAzyme, can be designed and synthesized for the detection of exosomes due to their great stability, sensitivity, and desirable manufacturing cost.[89] G4–hemin was often modified with aptamers at one end, thus the peroxidase activity of the DNAzyme can be affected by the folding and unfolding of the G-quadruplex motif upon the addition of exosomes carrying the target proteins.[82,86] The utilization of DNAzyme nanomaterials enabled the sensitive detection of exosomes at 10^2 par per µL level within a short reaction time, showing great potential in exosome-based early diagnostics of cancers.

4.3 Magnetic nanomaterials

Magnetic nanozymes such as Fe_3O_4 nanoparticles have become new solutions to exosome biosensors due to their superior pH and temperature stability, magnetic properties, and intrinsic HRP-mimicking ability.[90] Interestingly, the peroxidase activity of some magnetic nanozymes to TMB can be boosted 10-fold through the coating of long DNA.[47] Therefore, depending on the component, synthesis, and surface modification of the magnetic nanozymes, the biosensor developed can either be a sandwich-like immunoassay or a competitive reaction.

One of the major advantages of magnetic nanozyme is the sample-to-answer detection of exosomes without a pre-isolation step. In a colorimetric assay using gold-loaded ferric oxide nanocubes (Au-NPFe$_2$O$_3$NC), the nanozymes were functionalized with CD63 antibody and dispersed in bulk exosome samples for antigen capture (Fig. 5A). The exosomes-bound Au-NPFe$_2$O$_3$NC were then isolated directly through the magnet and transferred to tissue-specific antibody-coated electrodes for the formation of a typical sandwich structure through the nanozyme-catalyzed reaction. The UV-visible along with electrochemical quantification of exosomes were achieved with the oxidation of TMB. The assay achieved an extremely low LOD of 1 par per µL and a broad linear range of $1–10^4$ par per µL. Although the reaction took 4 hours to complete, it is 10 times more sensitive than NTA and demonstrated a satisfactory consistency (standard deviation < 5.5%).[91]

Apart from the sandwich-structured ELISA-like assays, magnetic nanozymes have also been incorporated into competitive bioassays.[90,92] An anion-exchange Fe_3O_4 nanoparticles (AE Fe_3O_4-NPs) were first proposed by Chen et al. for the direct isolation of exosomes from plasma (Fig. 5B).[90] The Fe_3O_4-NPs were capped with EpCAM, exhibiting an improved peroxidase activity. Through the competitive binding between exosome EpCAM and the nanozyme, the reduction of coated aptamers on the Fe_3O_4-NPs will lead to a decrease in catalytic activity and color change. This aptasensor can reach a LOD of 3.58×10^3 par per µL within 35 min, much faster than the existing visible detection methods. A linear range of $4.0 \times 10^4 – 6.0 \times 10^5$ par per µL was achieved for the direct detection of simulated exosome plasma samples.[90] Recently, another aptasensor for
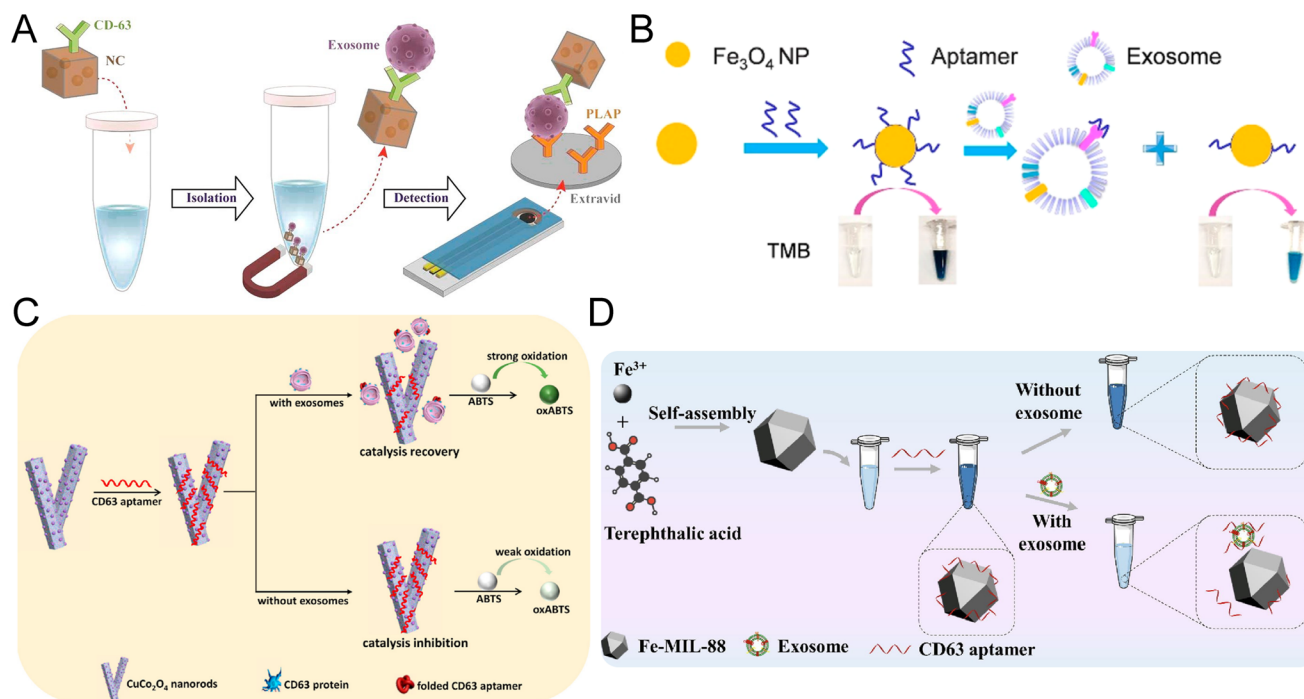
Fig. 5 Colorimetric biosensors developed based on magnetic nanomaterials and metal–organic frameworks. (A) Au-NPFe₂O₃NCs were applied as detection probes and enabled the direct isolation of exosomes. The complex was transferred to antibody-coated electrodes for the formation of a typical sandwich structure. Reproduced from ref. 91 with permission from the American Chemical Society, copyright 2019. (B) Fe₃O₄-NP-based competitive reaction for the detection of exosomes isolated through the anion exchange mechanism. Reproduced from ref. 90 with permission from the American Chemical Society, copyright 2018. (C) Colorimetric biosensor based on the release of CD63 aptamers from the CuCo₂O₄ nanorod surface in the presence of exosomes, resulting in the recovery of catalytic activity. Reproduced from ref. 98 with permission from Elsevier, copyright 2021. (D) Application of MOF nanozymes in a one-step reaction based on the regulation of Fe-MOFs through ssDNA. Reproduced from ref. 99 with permission from Elsevier, copyright 2022.

breast cancer exosomes was developed based on CD63 aptamer–iron oxide–copper ion nanozymes (Fe_3O_4–Cu^{2+}–NZs).[92] The presence of exosomes led to the conformational changes and dissociation of CD63 aptamers from Fe_3O_4–Cu^{2+}–NZs, resulting in a decrease in the peroxidase-like activity of the magnetic nanozyme. This aptasensor achieved a LOD of 5.91×10^3 par per µL with a linear range of 1.4×10^4–5.6×10^5 par per µL. However, the production of CD63 aptamer–Fe_3O_4–Cu^{2+}–NZs by non-homogeneous methods is technically complicated.

Generally, the magnetic properties of the magnetic nanozymes enable the rapid and convenient isolation of exosomes, facilitating different types of downstream analysis. This unique property is particularly advantageous for the reduction of operation procedure and reaction time for exosomes in complicated matrices such as plasma or serum. Like other 3-D nanoparticles, magnetic nanozymes offer enhanced sensitivity due to their large surface area, allowing for efficient capture. Meanwhile, the significant change of peroxidase activity upon the coating of DNA made them ideal components for the development of competitive biosensors.

4.4 Metal–organic frameworks (MOFs)

Metal–organic frameworks (MOFs) refer to porous coordination polymer materials that are made of metal ions bridged by organic ligands.[93] Researchers can deliberately manipulate the crystalline structure of MOFs through the selection of the organic and inorganic components, generating uniform nanoparticles with tunable pore sizes, and customizable chemical functionalities.[94] The high stability, biocompatibility, and oxidase-like activity of MOFs constructed in the past decade broadened the biomedical applications of this novel nanozyme, including drug delivery, cancer therapy, and diagnosis tests.[95–97]

Taking advantage of the target-responsive controllability of MOFs, a label-free biosensor of exosomes has been proposed (Fig. 5C).[98] Cu/Co bimetallic metal–organic frameworks ($CuCo_2O_4$ nanorods) were synthesized with highly dispersed and oxidase-like activity. In the preparation process, a nanorod-like Cu/Co bimetallic MOF was synthesized, which was applied as the template and transformed into $CuCo_2O_4$ nanorods after calcination in air. The detection system was built on the phenomenon that the adsorption of ssDNA inhibits the catalytic activity of $CuCo_2O_4$ nanorods by hindering the electron transfer between $CuCo_2O_4$ and ABTS. CD63 aptamers were employed to inhibit instead of strengthen the oxidase-like activity of $CuCo_2O_4$ nanorods without the presence of exosomes. As the exosome concentration increased, more CD63 aptamers would be released from the surface of

CuCo$_2$O$_4$ nanorods, resulting in the recovery of catalytic activity. The H$_2$O$_2$-free oxidation of ABTS generated a color change positively related to the concentration of target exosomes. This colorimetric assay was established over a range of 5.6×10^4 to 8.9×10^5 par per µL with an LOD of 4.5×10^3 par per µL, generating distinguishable signals between serum samples of cancer patients and healthy controls. Another recent study adopting the MOF nanozyme was based on the regulation of Fe-MOF by ssDNA, which is similar to that of magnetic nanozymes (Fig. 5D).[99] The specific absorbance between exosomes and CD63 aptamers downregulated the intrinsic peroxidase-like catalytic activity of the Fe-MOF under optimized conditions and achieved a LOD of 5.2×10^4 par per µL within extremely low reaction time (17 min). Relying on this one-step 'mixing-and-detection' procedure, exosomes of 1.1×10^5–2.2×10^7 par per µL could be detected. It is conceivable that such a rapid and convenient method would be favorable for commercial application in point-of-care diagnosis.

Despite the limited application of metal–organic frameworks (MOFs) in exosome detection, these porous materials possess high surface areas, tunable pore sizes, and diverse functionalization capabilities, making them ideal materials for the labeling-free capture and detection of exosomes. Great efforts have been made to investigate and compare the kinetic parameters of these MOFs and provide insight into the improvement of the analytical performance of exosome biosensors in the future.

4.5 Gold nanoparticles (AuNPs)

Gold nanoparticles along with peptide–gold nanoparticles (Pep–AuNPs) conjugates are typical nanozymes with intrinsic enzyme activity, substrate specificity, and biocompatibility.[100] Molecules with thiol functional groups can self-assemble to the AuNPs simultaneously through the S–Au bond, generating the surface layer for target recognition and catalysis.[101,102] AuNPs have been applied to the detection of exosome protein HIF-1α in an innovative study published by Wang et al.[103] The AuNPs were functionalized by HIF-1α aptamer, forming apt-AuNP-coated gold seeds. After exosomes were immobilized on the microplate, apt-AuNP-coated gold seeds were applied and grown by seed-mediated growth to increase the peroxidase mimicking property. Subsequently, the Au@Au core–shell nanoparticles catalyzed the TMB-based colorimetric reaction that quantified the exosome HIF-1α. With high system stability and low sample input (25 µL), the assay can reach a LOD of 0.2 ng L^{-1} and a linear range of 0.3–200 ng L^{-1} without preconcentration. Another nanozyme-assisted immunosorbent assay (NAISA) using AuNPs and lipid probes was reported soon after.[104] The exosomes were firstly engineered with DSPE-PEG-SH lipid anchor through hydrophobic interaction and then recognized by AuNPs automatically through the S–Au bond (forming Exo@Au). To quantify the expression level of exosome proteins for cancer diagnosis, antibodies specific for each protein target were seeded on a microplate for Exo@Au capture, and the Exo@Au nanozyme was used directly for the catalyzation of colorimetric reaction. This study demonstrates simplified detection procedures for multiple protein targets and a shorter reaction time (<3 h).

These two studies highlight the outstanding intrinsic enzyme activity of biocompatible AuNPs in colorimetric detection of exosome proteins. AuNPs demonstrate advantages in stability, mass-produced, and simplified operation procedures compared to conventional natural enzyme-based reactions. These research studies underscore the potential of AuNPs as a promising alternative to natural enzymes in the field of exosome detection and analysis.

Apart from the aforementioned studies that utilize the intrinsic enzyme activity of AuNPs, colorimetric detection of exosomes could also be achieved through the dispersion-to-aggregation change of AuNPs, exhibiting a red-to-blue color change as the concentration of exosomes varies.[105,106] Additionally, AuNPs and relevant nanomaterials have been applied to lateral flow immunoassays recently for the point-of-care testing of exosomes.[107–111] These two types of assays were reviewed in detail by Zhang et al., demonstrating the broad application range of AuNPs.[26]

5. Discussion

With the accumulation of knowledge regarding the important roles of exosomes in diagnosis and therapeutics, more attention has been paid to the rapid, sensitive, and convenient quantification of exosomes as a primary step for downstream applications.[1,112]

Over the past few decades, various advanced methods have been designed, and enzyme-based colorimetric detection of exosomes underwent rapid development in terms of convenience, sensitivity, and reaction efficiency. By observing the color change of the reaction, samples collected from cancer or healthy patients can be distinguished. To simplify the quantification of colorimetric signals, pH papers can be used instead of UV-spectrometry.[10,113] An alternative approach is to take photos through smartphones, collecting and transferring the test results with high-performance optical systems and the internet.[63] Currently, most colorimetric exosome biosensors can achieve a remarkable LOD range between 10^2 and 10^3 par per µL for complicated samples such as serum or plasma within 4–5 hours.[8,82,85,114] These improvements can be attributed to the fact that various high-affinity lipid-modified DNA anchors and several signal amplification methods (HCR, RCA) have been integrated into the assays.[9,30,35,50,104] Moreover, new nanomaterials such as CuSNPs,[115] CuONPs,[56] and AChE-loaded DNA microcapsules[11] were also synthesized and applied. The improved sensitivity and detection time demonstrate the great potential of these new methods in clinical applications where signal-collecting devices are not available or affordable.

While the performance and protocol of colorimetric immunoassays depend heavily on the nature properties of the enzymes, it is noteworthy to make a comparison between the advances in natural enzymes and nanozyme-based exosome

Table 3 Comparison of natural enzymes and nanozymes employed in colorimetric biosensors of exosomes

Enzyme	Mechanisms	Materials	Advantages	Disadvantages
Natural enzymes	Catalyze colorimetric reactions with stable activity and sandwich assays	Natural proteins such as HRP and ALP	Wide range of applications; suitable for multiple platforms; well-studied and commercially available; high catalytic activity; moderate reaction conditions; and convenient modification or labeling	Difficult for mass production; relatively expensive; low stability; limited types; and long reaction time
Nanozymes	Catalyze colorimetric reactions with adjustable activity; formation or disruption of nanozymes; competitive assays; and sandwich assays	Synthetic nanomaterials such as carbon nanomaterials, DNAzymes, magnetic nanomaterials, MOFs, and AuNPs	Diverse categories with unique characteristics; high stability; easy for mass production; low-cost; some have magnetic properties for rapid isolation; and shorter detection time	Commercially unavailable; limited integration into different platforms; slightly lower catalytic activity; poor biocompatibility; optimal temperature required; and difficult for modification or labeling

Abbreviations: HRP: horseradish peroxidase; ALP: alkaline phosphatase; MOFs; AuNPs: metal–organic frameworks; AuNPs: gold nanoparticles.

biosensors (Table 3). Therefore, a comprehensive analysis of their advantages, disadvantages, and challenges will be provided in the following sections.

5.1   Advantages and challenges of natural enzymes

As more and more novel detection platforms and nanozymes have been applied to the colorimetric detection of exosomes, different roles of the catalytic materials and unique biosensor designs can be found (Table 4). Natural enzymes have been widely applied in various fields due to their high catalytic activities and substrate specificity. One of the most important advantages of natural enzymes is the compatibility with various platforms such as microfluidics,[36,62–65] paper-based analytical devices (PADs),[34,54] and magnetic beads (MB).[8,9,35] These platforms enabled rapid isolation of exosomes, improved reaction efficiency, or convenient operation of the assays, boosting the performance of natural enzyme-based exosome biosensors.[116–120] What's more, natural enzymes are proteins that can be modified or labeled easily. SA-tagged HRP was frequently employed in other signal amplification methods (*i.e.* HCR, RCA) through SA–biotin interaction, fulfilling a dual signal amplification strategy that increases the sensitivity for exosome detection. The fact that natural enzymes retain their optimal catalytic activity at moderate temperatures (25–37 °C) made them suitable for assays without strict temperature control.

Nevertheless, natural enzymes also exhibit intrinsic limitations, such as instability and difficulty in mass production. They can be denatured during storage or upon environmental changes since their catalytic activity depends on the integrity of their native protein conformation; they can be digested by proteases, which are widely present and inevitable; although natural enzymes are commercially available, the synthesis and purification steps for high-quality enzymes are still time-consuming and expensive.[121,122] So far, the type of natural enzymes that are suitable for biomedical assays is limited. Therefore, a lot of effort has been made to discover new enzymes or extend the natural enzymes to enzyme mimetics in

the past decades. For the immunocapture of exosomes, the incubation with capture and detection probes will last for a longer time in a sandwich assay design. Therefore, the natural enzyme-based biosensors usually require a much longer reaction time compared to the nanozyme-based assays (Tables 1 and 2).

5.2   Advantages and challenges of nanozymes

Ever since the discovery of ferromagnetic NPs with peroxidase activity, the synthesis, characterization, and applications of nanozymes have attracted great attention from scientists in the field of biomedical science. In the past decade, a large number of studies on nanozyme-based exosome colorimetric biosensors emerged, demonstrating the advantages and challenges of these novel materials in this special application.

Generally, the 5 types of nanozymes listed in Table 4 harbor the following advantages compared with the traditional natural enzymes:

(1) Large diversity and distinct properties: although a limited number of nanozymes have been applied to the detection of exosomes, over 1200 nanozymes have been developed through rational design in the past 15 years, demonstrating great diversification and complexity.[39,123] In the aforementioned studies, each type of nanozyme offers unique advantages and catalytic properties. For example, DNAzymes themselves can contain aptamer sequences that facilitate the specific target protein binding, and undergo self-assembly upon favorable conditions.[77,80] Magnetic nanozymes were used for both exosome isolation and detection signal generation, leading to higher sensitivity and a simple sample-to-answer operation procedure. Therefore, despite the variations in enzymatic activities of the nanozymes, each type of these novel materials harbors distinct properties that could meet the specific goal of the novel detection techniques. In comparison, natural enzymes employed in colorimetric detection methods are predominantly limited to horseradish peroxidase (HRP), which is also the most frequently used enzyme in research, clinical diagnosis, and industry.

Table 4 Summarization of nanozymes employed in colorimetric biosensors of exosomes

Nanozyme	Characteristics and advantages	Limitations	Reaction principle	Ref.
Carbon nanomaterials	Various morphologies with different dimensions; easy to functionalize with ssDNA; high conductivity and low electron transfer resistance; reusable and low-cost	Tend to aggregate and low solubility in water	Competitive reaction through affinity binding of ssDNA (aptamer)	73 and 74
DNAzymes	Adjustable activity and stability through molecular interaction; high bioactivity and catalytic efficiency; also function as aptamers; and high specificity	Require strict storage conditions; sensitive to the reaction environment; few active sites; and temperature control required	Competitive reaction affects the formation of hemin/G-quadruplex DNAzyme and affinity binding of the DNAzyme linked aptamer	82 and 86
Magnetic nanomaterials	Magnetism and easy for collection; pre-isolation free; easy to functionalize with ssDNA; easy to recover and concentrate; reusable and low-cost	Temperature control required	Competitive reaction through affinity binding of ssDNA (aptamer) and labeled with specific detection antibody	90–92
Metal–organic frameworks	Hierarchical porous structures; adjustable element content and pore size; large surface area-volume ratio; and easy to functionalize	Stringent synthesis protocol and conditions; relatively expensive; and temperature control required	Competitive reaction through affinity binding of ssDNA (aptamer)	98 and 99
Gold nanoparticles	Natural adsorption for biomolecules; adjustable catalytic performance through particle size; and easy to synthesise	Stringent control of particle size and temperature control required	Binding to the modified exosome membrane through lipid probes and labeled with aptamers	103 and 104

(2) High stability and durability: nanozymes generally exhibit superior thermal stability and durability compared to natural enzymes. Most nanozymes are nanoparticles of uniform chemical composition, demonstrating a remarkable resilience to changes in their external chemical conditions. Except for DNAzymes, most nanozymes are resistant to the biological digestion of protease or DNase, which are widely present in biological samples and environments. The shelf life of the DNAzymes in their powder form can also be long if an appropriate temperature is kept. This enhanced stability ensures the long-term storage of nanozymes without compromising their catalytic activity, as well as the robustness of nanozyme-based biosensors.

(3) Low cost of nanozyme and assays: as alternatives to natural enzymes, nanozymes were created through artificial approaches with metal ions, carbon, nucleotides, and other organic materials. Therefore, once the components and synthetic strategies are fixed, they can be produced easily with inexpensive equipment. Unlike natural enzymes which require tagging and purification during production, nanozymes can be synthesized and modified at much lower costs. Additionally, the fact that many nanozyme-based biosensors adopted a competitive assay design further reduces the expenditure for expensive antibodies used in the biosensors. Some nanozymes can also be recycled, as the change of peroxidase or oxidase activity of the nanomaterials through reversible surface modification is only temporary. All these characteristics could contribute to cost reduction, making nanozymes and nanozyme-based biosensors particularly advantageous for biomedical applications and commercialization.

(4) Adjustable enzymatic activity: compared to natural enzymes, nanozymes have a large surface area-to-volume ratio, facilitating their surface modification and conjugation with other functional groups. For the nanoparticles, most catalytic reactions occur on the surface where the activation energy of the substrates can be lowered through electron transfer or conformational change.[124,125] Thus, surface modification can influence biocompatibility, solubility, and most importantly, their catalytic activities.[126,127] It has been reported that Fe_3O_4 nanozymes modified with histidine on the surface exhibited a 10-fold increase in binding affinity for H_2O_2 and a 20-fold higher peroxidase activity compared to the naked ones.[46] The regulation of nanozyme activity through biomolecules that participate in the reaction has promoted the invention of various new biosensors of exosomes.

(5) Simplified and faster reaction: unlike natural enzymes which are typically labeled on the detection probes in a sandwich-structured assay, nanozymes are frequently integrated into label-free competitive reactions.[11,73,74,86,90,92,98,99] Without the capture step which is generally time-consuming for exosome nanoparticles, the reaction time can be shortened. These colorimetric assays are conducted by incubation of the nanozyme directly with the exosomes, followed by the addition of substrates for signal generation. Due to the reduction of the capture process and multiple steps for signal amplification, a significantly shorter detection time was achieved.[73,74,90] A remarkable detection time of 17 min was achieved for a Fe-MOF-based label-free biosensor due to its streamlined and straightforward procedure.[99] In contrast, exosome detection based on natural enzymes and nanozymes with sandwich-structured assays typically lasts for several hours, unable to meet the point-of-care need.

Despite the aforementioned advantages, nanozymes are also facing the following challenges at the current stage compared with the widely applied natural enzymes:

(1) Study of the biochemical properties is inadequate: due to their recent emergence and the distinct composition of the nanozymes, investigation of their biochemical properties is

generally inadequate. Some studies characterized the optimal temperature, pH, substrate concentration, and reaction buffer of the specific nanozyme, but their preferred condition in the complicated matrix such as serum or saliva was not investigated compared to well-established natural enzymes. Since most nanozymes are synthetic materials that vary in format, size, chemical component, or catalytic site, more research regarding their reaction mechanisms and matching conditions is preferred to further elevate their enzymatic activity.

(2) Special temperature control is required: nanozymes exhibit more stringent temperature requirements in comparison to traditional natural enzymes. While natural enzymes typically operate optimally from room temperature to around 37 °C, some nanozymes used for exosome detection showed a distinct and narrow range of reaction temperatures that is higher than room temperature.[87] This issue hinders the further development of nanozyme-based colorimetric biosensors into a real point-of-care test for all kinds of scenarios. Since the catalytic ability of each nanoparticle can be adjusted through synthetic strategies, maybe the desired functional temperature can be controlled through computational chemistry or artificial intelligence-assisted rational design in future studies.[39]

(3) Different levels of production scale: synthesis of DNAzymes and gold nanoparticles are relatively mature and affordable, but some types of nanozymes have not been verified on a large scale, long term, or made commercially available. For example, the synthesis of MOFs with outstanding performance is notably complicated due to the intricate, multi-step processes and precise temperature control required. Therefore, the scale-up of nanozymes production in laboratory settings can be very difficult, hindering the broad investigation and application of nanozymes in various fields.

(4) Limited incorporation into multiple platforms: currently, nanozyme-based colorimetric detections are predominantly performed within test tubes, offering limited versatility and convenience. Natural enzymes, on the other hand, have demonstrated great adaptability and have been integrated into various platforms such as microfluidic and PADs, enhancing the overall performance of biosensors through external facilities.[34,36,62] The limited incorporation of nanozyme in other platforms might be a reflection of the early stage of this field. For example, whether there will be nonspecific absorbance of nanoparticles on the microfluidic chip surface should be investigated before application. Since some nanozymes are temperature-sensitive for their maximum catalytic activity, platforms without precise temperature control (such as PADs) may not be suitable for nanozyme-based assays. It may also be possible that sophisticated surface modification is needed for the functionalization of some nanozymes before they can be integrated into other platforms. By all means, we would expect more and more types of nanozymes to be adopted in diverse technologies in the future.

Generally, it is not easy to compare the performance like detection limitation or sensitivity of natural enzyme and nanozyme, because they detected different targets and used disparate recognition probes. In biosensors based on natural enzymes, antibodies are frequently used, whereas in assays using nanozymes, aptamers are more commonly utilized due to their high affinity for ssDNA. Even with the same antibodies, the results also cannot be compared directly because the affinity of antibodies from different manufacturers and batches varies, which will impact the test results. A rigorous evaluation of the performance of the two enzymes needs to be performed in a system that uses the same recognition elements and surface protein as the target. These important investigations are needed in the future.

6. Conclusion and future perspectives

Exosomes present in various bodily fluids hold strong potential in liquid biopsy and early diagnosis. Colorimetric detection methods have been utilized for the detection of exosomes due to the convenience of signal readout, involving both natural enzymes and novel nanozymes. The rapid development of nanozymes in the past decade introduced a new direction in the colorimetric detection of exosomes, improving biosensors in terms of sensitivity, convenience, reaction time, and cost. This comprehensive review provides insights into the current state-of-the-art colorimetric detection methods for exosomes, categorizing them into natural enzyme-based and nanozyme-based colorimetric biosensors, highlighting the great potential of nanozymes in advancing exosome detection technologies.

In future studies, improvements are still required for both enzyme-based and nanozyme-based exosome biosensors. For natural enzymes, efforts can be made to engineer the nano and microscale environments around enzymes and their active sites. Polymerization of the HRP molecules already becomes a well-accepted approach for the boosting of signals.[128] Thus, we would expect this polymeric horseradish peroxidase (Poly-HRP) material to be verified in the colorimetric biosensors of exosomes, enhancing the sensitivity of assays. For nanozymes, extensive investigations are still required to fully explore their capabilities and optimize their performance. Although nanozymes hold the potential for mass production, it is still essential to establish a robust scale-up system for industrial production and verify the stability of nanozymes under such conditions. These efforts will be vital for the long-term development of the field, enabling the wide utilization of nanozymes in various applications. What's more, the integration of nanozymes into diverse platforms such as microfluidics and paper-based devices is an alternative approach to further improve the performance of nanozyme-based colorimetric biosensors. The future will witness increased breakthroughs in nanozyme technology and the emergence of novel biocatalysts that could overcome the above-mentioned and other potential challenges.[10] These advanced materials and designs of exosome colorimetric biosensors will further bring about the broad application of exosome-based diagnosis in the future.

Author contributions

Conflicts of interest

The authors declare no conflict of interest.

Acknowledgements

References

1 R. Kalluri and V. S. LeBleu, *Science*, 2020, **367**, eaau6977.
2 R. Isaac, F. C. G. Reis, W. Ying and J. M. Olefsky, *Cell Metab.*, 2021, **33**, 1744–1762.
3 C. Li, Y. Q. Ni, H. Xu, Q. Y. Xiang, Y. Zhao, J. K. Zhan, J. Y. He, S. Li and Y. S. Liu, *Signal Transduction Targeted Ther.*, 2021, **6**, 383.
4 D. Yu, Y. Li, M. Wang, J. Gu, W. Xu, H. Cai, X. Fang and X. Zhang, *Mol. Cancer*, 2022, **21**, 56.
5 L. Zhao, H. Wang, J. Fu, X. Wu, X. Y. Liang, X. Y. Liu, X. Wu, L. L. Cao, Z. Y. Xu and M. Dong, *Biosens. Bioelectron.*, 2022, **214**, 114487.
6 N. Cheng, D. Du, X. Wang, D. Liu, W. Xu, Y. Luo and Y. Lin, *Trends Biotechnol.*, 2019, **37**, 1236–1254.
7 S. Gurunathan, M. H. Kang, M. Jeyaraj, M. Qasim and J. H. Kim, *Cells*, 2019, **8**, 307.
8 R. Zeng, J. Wang, Q. Wang, D. Tang and Y. Lin, *Talanta*, 2021, **221**, 121600.
9 C. Li, M. Zhou, H. Wang, J. Wang and L. Huang, *Talanta*, 2022, **245**, 123444.
10 Y. Yang, C. Li, H. Shi, T. Chen, Z. Wang and G. Li, *Talanta*, 2019, **192**, 325–330.
11 X. Shen, S. Wang, Q. Lu, Y. Guo and L. Qian, *Anal. Chim. Acta*, 2022, **1192**, 339357.
12 T. Zhang, S. Ma, J. Lv, X. Wang, H. K. Afewerky, H. Li and Y. Lu, *Ageing Res. Rev.*, 2021, **68**, 101321.
13 C. Z. J. Lim, Y. Zhang, Y. Chen, H. Zhao, M. C. Stephenson, N. R. Y. Ho, Y. Chen, J. Chung, A. Reilhac, T. P. Loh, C. L. H. Chen and H. Shao, *Nat. Commun.*, 2019, **10**, 1144.
14 R. Xu, A. Rai, M. Chen, W. Suwakulsiri, D. W. Greening and R. J. Simpson, *Nat. Rev. Clin Oncol.*, 2018, **15**, 617–638.
15 G. Raposo and W. Stoorvogel, *J. Cell Biol.*, 2013, **200**, 373–383.
16 H. Shao, H. Im, C. M. Castro, X. Breakefield, R. Weissleder and H. Lee, *Chem. Rev.*, 2018, **118**, 1917–1950.
17 E. Serrano-Pertierra, M. Oliveira-Rodriguez, M. Matos, G. Gutierrez, A. Moyano, M. Salvador, M. Rivas and M. C. Blanco-Lopez, *Biomolecules*, 2020, **10**, 824.
18 E. van der Pol, F. A. Coumans, A. E. Grootemaat, C. Gardiner, I. L. Sargent, P. Harrison, A. Sturk, T. G. van Leeuwen and R. Nieuwland, *J. Thromb. Haemostasis*, 2014, **12**, 1182–1192.
19 R. Szatanek, M. Baj-Krzyworzeka, J. Zimoch, M. Lekka, M. Siedlar and J. Baran, *Int. J. Mol. Sci.*, 2017, **18**, 1153.
20 S. Salunkhe, Dheeraj, M. Basak, D. Chitkara and A. Mittal, *J. Controlled Release*, 2020, **326**, 599–614.
21 J. He, W. Ren, W. Wang, W. Han, L. Jiang, D. Zhang and M. Guo, *Drug Delivery Transl. Res.*, 2022, **12**, 2385–2402.
22 S. D. Gan and K. R. Patel, *J. Invest. Dermatol.*, 2013, **133**, e12.
23 Q. Zhao, D. Lu, G. Zhang, D. Zhang and X. Shi, *Talanta*, 2021, **223**, 121722.
24 L. Gao, J. Zhuang, L. Nie, J. Zhang, Y. Zhang, N. Gu, T. Wang, J. Feng, D. Yang, S. Perrett and X. Yan, *Nat. Nanotechnol.*, 2007, **2**, 577–583.
25 Y. Song, W. Wei and X. Qu, *Adv. Mater.*, 2011, **23**, 4215–4236.
26 L. Zhang, C. Gu, J. Wen, G. Liu, H. Liu and L. Li, *Anal. Bioanal. Chem.*, 2021, **413**, 83–102.
27 D. Jiang, D. Ni, Z. T. Rosenkrans, P. Huang, X. Yan and W. Cai, *Chem. Soc. Rev.*, 2019, **48**, 3683–3704.
28 B. Shao and Z. Xiao, *Anal. Chim. Acta*, 2020, **1114**, 74–84.
29 C. Zhu, L. Li, Z. Wang, M. Irfan and F. Qu, *Biosens. Bioelectron.*, 2020, **160**, 112213.
30 J. Zheng, X. Hu, Y. Zeng, B. Zhang, Z. Sun, X. Liu, W. Zheng and Y. Chai, *Anal. Chim. Acta*, 2023, **1263**, 341319.
31 H. Xiong, Z. Huang, Z. Yang, Q. Lin, B. Yang, X. Fang, B. Liu, H. Chen and J. Kong, *Small*, 2021, **17**, e2007971.
32 H. Yang, C. S. Bever, H. Zhang, G. M. Mari, H. Li, X. Zhang, L. Guo, Z. Wang, P. Luo and Z. Wang, *Anal. Biochem.*, 2019, **581**, 113336.

33 B. J. Ryan, N. Carolan and C. O'Fagain, *Trends Biotechnol.*, 2006, **24**, 355–363.

34 C. H. Lai, C. L. Lee, C. A. Vu, V. T. Vu, Y. H. Tsai, W. Y. Chen and C. M. Cheng, *Front. Bioeng. Biotechnol.*, 2022, **10**, 836082.

35 F. He, H. Liu, X. Guo, B. C. Yin and B. C. Ye, *Anal. Chem.*, 2017, **89**, 12968–12975.

36 Z. Chen, S. B. Cheng, P. Cao, Q. F. Qiu, Y. Chen, M. Xie, Y. Xu and W. H. Huang, *Biosens. Bioelectron.*, 2018, **122**, 211–216.

37 Z. Huang, Q. Lin, X. Ye, B. Yang, R. Zhang, H. Chen, W. Weng and J. Kong, *Talanta*, 2020, **218**, 121089.

38 H. Wei and E. Wang, *Chem. Soc. Rev.*, 2013, **42**, 6060–6093.

39 Z. Chen, Y. Yu, Y. Gao and Z. Zhu, *ACS Nano*, 2023, **17**, 13062–13080.

40 Y. Wang and Y. Xianyu, *Small Methods*, 2022, **6**, e2101576.

41 Y. Huang, J. Ren and X. Qu, *Chem. Rev.*, 2019, **119**, 4357–4412.

42 J. Mujtaba, J. Liu, K. K. Dey, T. Li, R. Chakraborty, K. Xu, D. Makarov, R. A. Barmin, D. A. Gorin, V. P. Tolstoy, G. Huang, A. A. Solovev and Y. Mei, *Adv. Mater.*, 2021, **33**, e2007465.

43 H. Y. Shin, T. J. Park and M. I. Kim, *J. Nanomater.*, 2015, **2015**, 1–11.

44 N. Stasyuk, O. Smutok, O. Demkiv, T. Prokopiv, G. Gayda, M. Nisnevitch and M. Gonchar, *Sensors*, 2020, **20**, 4509.

45 A. A. Vernekar, T. Das, S. Ghosh and G. Mugesh, *Chem.–Asian J.*, 2016, **11**, 72–76.

46 K. Fan, H. Wang, J. Xi, Q. Liu, X. Meng, D. Duan, L. Gao and X. Yan, *Chem. Commun.*, 2016, **53**, 424–427.

47 B. Liu and J. Liu, *Nanoscale*, 2015, **7**, 13831–13835.

48 J. Wu, X. Wang, Q. Wang, Z. Lou, S. Li, Y. Zhu, L. Qin and H. Wei, *Chem. Soc. Rev.*, 2019, **48**, 1004–1076.

49 M. Logozzi, A. De Milito, L. Lugini, M. Borghi, L. Calabro, M. Spada, M. Perdicchio, M. L. Marino, C. Federici, E. Iessi, D. Brambilla, G. Venturi, F. Lozupone, M. Santinami, V. Huber, M. Maio, L. Rivoltini and S. Fais, *PLoS One*, 2009, **4**, e5219.

50 Y. Xia, T. Chen, G. Chen, Y. Weng, L. Zeng, Y. Liao, W. Chen, J. Lan, J. Zhang and J. Chen, *Talanta*, 2020, **214**, 120851.

51 C. Gohner, M. Weber, D. S. Tannetta, T. Groten, T. Plosch, M. M. Faas, S. A. Scherjon, E. Schleussner, U. R. Markert and J. S. Fitzgerald, *Am. J. Reprod. Immunol.*, 2015, **73**, 582–588.

52 D. R. Hristov, C. Rodriguez-Quijada, J. Gomez-Marquez and K. Hamad-Schifferli, *Sensors*, 2019, **19**, 554.

53 S. Smith, J. G. Korvink, D. Mager and K. Land, *RSC Adv.*, 2018, **8**, 34012–34034.

54 C. Chen, B. R. Lin, M. Y. Hsu and C. M. Cheng, *J. Visualized Exp.*, 2015, e52722, DOI: **10.3791/52722**.

55 S. Jiawei, C. Zhi, T. Kewei and L. Xiaoping, *Front. Bioeng. Biotechnol.*, 2022, **10**, 942077.

56 Y. Xia, T. Chen, W. Chen, G. Chen, L. Xu, L. Zhang, X. Zhang, W. Sun, J. Lan, X. Lin and J. Chen, *Anal. Chim. Acta*, 2022, **1191**, 339279.

57 F. He, J. Wang, B. C. Yin and B. C. Ye, *Anal. Chem.*, 2018, **90**, 8072–8079.

58 J. Zheng, X. Hu, Y. Zeng, B. Zhang, Z. Sun, X. Liu, W. Zheng and Y. Chai, *Anal. Chim. Acta*, 2023, **1263**, 341319.

59 Y. Wan, G. Cheng, X. Liu, S. J. Hao, M. Nisic, C. D. Zhu, Y. Q. Xia, W. Q. Li, Z. G. Wang, W. L. Zhang, S. J. Rice, A. Sebastian, I. Albert, C. P. Belani and S. Y. Zheng, *Nat. Biomed. Eng.*, 2017, **1**, 0058.

60 Y. Xiong, L. He, M. Yang, Y. Wang, X. Liu, S. Ma, B. Yang and F. Guan, *Sens. Actuators, B*, 2022, **353**, 131126.

61 L. Xu, R. Chopdat, D. Li and K. T. Al-Jamal, *Biosens. Bioelectron.*, 2020, **169**, 112576.

62 R. Vaidyanathan, M. Naghibosadat, S. Rauf, D. Korbie, L. G. Carrascosa, M. J. Shiddiky and M. Trau, *Anal. Chem.*, 2014, **86**, 11125–11132.

63 L. G. Liang, M. Q. Kong, S. Zhou, Y. F. Sheng, P. Wang, T. Yu, F. Inci, W. P. Kuo, L. J. Li, U. Demirci and S. Wang, *Sci. Rep.*, 2017, **7**, 46224.

64 H. K. Woo, V. Sunkara, J. Park, T. H. Kim, J. R. Han, C. J. Kim, H. I. Choi, Y. K. Kim and Y. K. Cho, *ACS Nano*, 2017, **11**, 1360–1370.

65 W. Chen, H. Li, W. Su and J. Qin, *Biomicrofluidics*, 2019, **13**, 054113.

66 M. N. Le and Z. H. Fan, *Biomed. Mater.*, 2021, **16**, 022005.

67 J. C. Contreras-Naranjo, H. J. Wu and V. M. Ugaz, *Lab Chip*, 2017, **17**, 3558–3577.

68 Y. Huang, J. Ren and X. Qu, *Chem. Rev.*, 2019, **119**, 4357–4412.

69 C. Zhu, Z. Zeng, H. Li, F. Li, C. Fan and H. Zhang, *J. Am. Chem. Soc.*, 2013, **135**, 5998–6001.

70 Q. Wang, W. Wang, J. Lei, N. Xu, F. Gao and H. Ju, *Anal. Chem.*, 2013, **85**, 12182–12188.

71 N. L. Teradal and R. Jelinek, *Adv. Healthc. Mater.*, 2017, **6**, 1700574.

72 M. S. Hizir, M. Top, M. Balcioglu, M. Rana, N. M. Robertson, F. Shen, J. Sheng and M. V. Yigit, *Anal. Chem.*, 2016, **88**, 600–605.

73 Y. Xia, M. Liu, L. Wang, A. Yan, W. He, M. Chen, J. Lan, J. Xu, L. Guan and J. Chen, *Biosens. Bioelectron.*, 2017, **92**, 8–15.

74 Y. M. Wang, J. W. Liu, G. B. Adkins, W. Shen, M. P. Trinh, L. Y. Duan, J. H. Jiang and W. Zhong, *Anal. Chem.*, 2017, **89**, 12327–12333.

75 D. A. Heller, H. Jin, B. M. Martinez, D. Patel, B. M. Miller, T.-K. Yeung, P. V. Jena, C. Höbartner, T. Ha, S. K. Silverman and M. S. Strano, *Nat. Nanotechnol.*, 2008, **4**, 114–120.

76 Y. Song, X. Wang, C. Zhao, K. Qu, J. Ren and X. Qu, *Chem. – Eur. J.*, 2010, **16**, 3617–3621.

77 S. Khan, B. Burciu, C. D. M. Filipe, Y. Li, K. Dellinger and T. F. Didar, *ACS Nano*, 2021, **15**, 13943–13969.

78 J. Jouha and H. Xiong, *Small*, 2021, **17**, e2105439.

79 I. Cozma, E. M. McConnell, J. D. Brennan and Y. Li, *Biosens. Bioelectron.*, 2021, **177**, 112972.

80 E. Golub, H. B. Albada, W. C. Liao, Y. Biniuri and I. Willner, *J. Am. Chem. Soc.*, 2016, **138**, 164–172.

81 A. Shimizu, H. Nishiumi, Y. Okumura and K. Watanabe, *J. Affective Disord.*, 2015, **179**, 175–182.

82 Y. Zhou, H. Xu, H. Wang and B. C. Ye, *Analyst*, 2019, **145**, 107–114.

83 G. Pelossof, R. Tel-Vered, J. Elbaz and I. Willner, *Anal. Chem.*, 2010, **82**, 4396–4402.

84 D. Chang, S. Zakaria, M. Deng, N. Allen, K. Tram and Y. Li, *Sensors*, 2016, **16**, 2061.

85 Y. Zhou, H. Xu, H. Wang and B.-C. Ye, *Analyst*, 2020, **145**, 107–114.

86 J. Kuang, Z. Fu, X. Sun, C. Lin, S. Yang, J. Xu, M. Zhang, H. Zhang, F. Ning and P. Hu, *Analyst*, 2022, **147**, 5054–5061.

87 W. Cheng, Y. Yao, D. Li, C. Duan, Z. Wang and Y. Xiang, *Biosens. Bioelectron.*, 2023, **238**, 115552.

88 M. Deng, D. Zhang, Y. Zhou and X. Zhou, *J. Am. Chem. Soc.*, 2008, **130**, 13095–13102.

89 R. Hu, T. Liu, X.-B. Zhang, Y. Yang, T. Chen, C. Wu, Y. Liu, G. Zhu, S. Huan, T. Fu and W. Tan, *Anal. Chem.*, 2015, **87**, 7746–7753.

90 J. Chen, Y. Xu, Y. Lu and W. Xing, *Anal. Chem.*, 2018, **90**, 14207–14215.

91 K. Boriachek, M. K. Masud, C. Palma, H. P. Phan, Y. Yamauchi, M. S. A. Hossain, N. T. Nguyen, C. Salomon and M. J. A. Shiddiky, *Anal. Chem.*, 2019, **91**, 3827–3834.

92 J. Long, F. Wang, G. Zha, K. Che, J. Luo and Z. Deng, *J. Biomed. Nanotechnol.*, 2022, **18**, 1084–1096.

93 O. M. Yaghi, M. O'Keeffe, N. W. Ockwig, H. K. Chae, M. Eddaoudi and J. Kim, *Nature*, 2003, **423**, 705–714.

94 Y. Sakata, S. Furukawa, M. Kondo, K. Hirai, N. Horike, Y. Takashima, H. Uehara, N. Louvain, M. Meilikhov, T. Tsuruoka, S. Isoda, W. Kosaka, O. Sakata and S. Kitagawa, *Science*, 2013, **339**, 193–196.

95 S. Wang, C. M. McGuirk, A. d'Aquino, J. A. Mason and C. A. Mirkin, *Adv. Mater.*, 2018, **30**, e1800202.

96 M.-X. Wu and Y.-W. Yang, *Adv. Mater.*, 2017, **29**, 1606134.

97 L. Ma, F. Jiang, X. Fan, L. Wang, C. He, M. Zhou, S. Li, H. Luo, C. Cheng and L. Qiu, *Adv. Mater.*, 2020, **32**, e2003065.

98 Y. Zhang, Q. Su, D. Song, J. Fan and Z. Xu, *Anal. Chim. Acta*, 2021, **1145**, 9–16.

99 Z. Ding, Y. Lu, Y. Wei, D. Song, Z. Xu and J. Fang, *J. Colloid Interface Sci.*, 2022, **612**, 424–433.

100 D. J. Mikolajczak, A. A. Berger and B. Koksch, *Angew. Chem., Int. Ed.*, 2020, **59**, 8776–8785.

101 E. Pensa, E. Cortés, G. Corthey, P. Carro, C. Vericat, M. H. Fonticelli, G. Benítez, A. A. Rubert and R. C. Salvarezza, *Acc. Chem. Res.*, 2012, **45**, 1183–1192.

102 T. Taguchi, K. Isozaki and K. Miki, *Adv. Mater.*, 2012, **24**, 6462–6467.

103 Q. L. Wang, W. X. Huang, P. J. Zhang, L. Chen, C. K. Lio, H. Zhou, L. S. Qing and P. Luo, *Mikrochim. Acta*, 2019, **187**, 61.

104 H. Di, Z. Mi, Y. Sun, X. Liu, X. Liu, A. Li, Y. Jiang, H. Gao, P. Rong and D. Liu, *Theranostics*, 2020, **10**, 9303–9314.

105 W. Liu, J. Li, Y. Wu, S. Xing, Y. Lai and G. Zhang, *Biosens. Bioelectron.*, 2018, **102**, 204–210.

106 Y. Jiang, M. Shi, Y. Liu, S. Wan, C. Cui, L. Zhang and W. Tan, *Angew. Chem., Int. Ed.*, 2017, **56**, 11916–11920.

107 N. Cheng, Y. Song, Q. Shi, D. Du, D. Liu, Y. Luo, W. Xu and Y. Lin, *Anal. Chem.*, 2019, **91**, 13986–13993.

108 Q. Yu, Q. Zhao, S. Wang, S. Zhao, S. Zhang, Y. Yin and Y. Dong, *Anal. Biochem.*, 2020, **594**, 113591.

109 M. Oliveira-Rodriguez, S. Lopez-Cobo, H. T. Reyburn, A. Costa-Garcia, S. Lopez-Martin, M. Yanez-Mo, E. Cernuda-Morollon, A. Paschen, M. Vales-Gomez and M. C. Blanco-Lopez, *J. Extracell. Vesicles*, 2016, **5**, 31803.

110 S. Lopez-Cobo, C. Campos-Silva, A. Moyano, M. Oliveira-Rodriguez, A. Paschen, M. Yanez-Mo, M. C. Blanco-Lopez and M. Vales-Gomez, *J. Nanobiotechnol.*, 2018, **16**, 47.

111 M. Oliveira-Rodriguez, E. Serrano-Pertierra, A. C. Garcia, S. Lopez-Martin, M. Yanez-Mo, E. Cernuda-Morollon and M. C. Blanco-Lopez, *Biosens. Bioelectron.*, 2017, **87**, 38–45.

112 W. Yu, J. Hurley, D. Roberts, S. K. Chakrabortty, D. Enderle, M. Noerholm, X. O. Breakefield and J. K. Skog, *Ann. Oncol.*, 2021, **32**, 466–477.

113 X. Shen, S. Wang, Q. Lu, Y. Guo and L. Qian, *Anal. Chim. Acta*, 2022, **1192**, 339357.

114 J. Long, F. Wang, G. Zha, K. Che, J. Luo and Z. Deng, *J. Biomed. Nanotechnol.*, 2022, **18**, 1084–1096.

115 S. Chen, T. Jiang, H. Lin, J. Chen, S. Yang, P. Wang, X. Gan, Y. Wang, B. Xu, J. Sun, C. Yin, Z. Huang and Y. Fang, *Anal. Chem.*, 2021, **93**, 10372–10377.

116 B. Chutvirasakul, N. Nuchtavorn, L. Suntornsuk and Y. Zeng, *Electrophoresis*, 2020, **41**, 311–318.

117 S. Kasetsirikul, K. T. Tran, K. Clack, N. Soda, M. J. A. Shiddiky and N. T. Nguyen, *Analyst*, 2022, **147**, 3732–3740.

118 S. T. Sanjay, M. Li, W. Zhou, X. Li and X. Li, *Microsyst. Nanoeng.*, 2020, **6**, 28.

119 S. Lin, Z. Yu, D. Chen, Z. Wang, J. Miao, Q. Li, D. Zhang, J. Song and D. Cui, *Small*, 2020, **16**, e1903916.

120 B. Lin, Y. Lei, J. Wang, L. Zhu, Y. Wu, H. Zhang, L. Wu, P. Zhang and C. Yang, *Small Methods*, 2021, **5**, e2001131.

121 J. M. Zen and A. S. Kumar, *Acc. Chem. Res.*, 2001, **34**, 772–780.

122 G. Wulff, *Chem. Rev.*, 2002, **102**, 1–28.

123 M. Wei, J. Lee, F. Xia, P. Lin, X. Hu, F. Li and D. Ling, *Acta Biomater.*, 2021, **126**, 15–30.

124 S. Garehbaghi, A. M. Ashrafi, V. Adam and L. Richtera, *Mater. Today Bio*, 2023, **20**, 100656.

125 W. Liang, P. Wied, F. Carraro, C. J. Sumby, B. Nidetzky, C. K. Tsung, P. Falcaro and C. J. Doonan, *Chem. Rev.*, 2021, **121**, 1077–1129.

126 X. Ding, Z. Zhao, Y. Zhang, M. Duan, C. Liu and Y. Xu, *Small*, 2023, **19**, e2207142.

127 W. Mei, W. Huang, X. Liu, H. Wang, Q. Wang, X. Yang and K. Wang, *Anal. Chem.*, 2023, **95**, 11391–11398.

128 L. Lancaster, W. Abdallah, S. Banta and I. Wheeldon, *Chem. Soc. Rev.*, 2018, **47**, 5177–5186.